

1 Revision on interactive comment on “ The contribution of tephra constituents
2 during biogenic silica determination: implications for soil and paleoecological
3 studies” by W. Clymans et. al.

4
5 Dear Editor,

6
7 We are pleased that both reviewers and associate editor support publication and
8 acknowledge the importance of our study. We have complied with all their
9 requests, and where not, reasoning is detailed accordingly (see below). We hope
10 the revised manuscript is ready for publication. Please feel free to contact us if
11 additional explanations or revisions are necessary.

12 Kind Regards,
13 Wim Clymans and co-authors

14
15 **Referee #1: D.J. Lowe**

16 The authors are pleased to receive positive comments on the relevance, content
17 and writing style from D.J. Lowe (an expert within the field). His detailed
18 suggestions to improve technical and language issues enhanced clarity and led to
19 more correct presentation of the results. We greatly appreciated his annotated
20 MS .

21
22 **Referee #2: Anonymous**

23 The only critical comments that are made deal with the generality of the study:
24 *Guidelines are good for caveats involved in volcanic soils, but one can question
25 if general observations can be applied to other soils samples.

26 *Impact of the paper is restricted to specific samples from which the role in a
27 global context is quite small.

28 *We agree with the reviewer that we had to tone down some of our statements with
29 respect to the generality of our results. However, we want to stress that although
30 having a small spatial distribution, volcanic soils are suggested to coincide with an
31 important biological control on the Si cycle (Derry et al., 2005 & Meunier et al.,
32 1998). Therefore, those systems have received increased attention as being highly
33 relevant systems to study the effect of biology on the Si cycle. Our observation that
34 the non-biogenic fraction can significantly contribute to the Si_{Alk} pool is also
35 observed in other soil systems (see Barão et al., 2014. EJSS; Barão et al., 2015.
36 LOM), and has equally important consequences for the interpretation of the BSi
37 pool. This supports the relevance of our general observation with respect to
38 increased critical interpretation of BSi estimates in soil profiles, and certainly in
39 volcanic prone areas.*

40
41 C1: Add a short description of sampling method and preservation for the
42 samples referenced as unpublished data in Table 1.

43 *For unpublished data a short description with basic information was added in the
44 caption of table 1. Notice that we have changed the representation of the ages as
45 some of them where not cal BP dates.*

46
47 C2: Dampen following statement: “We formulate guidelines for the use of
48 alkaline extraction techniques to determine BSi in soils and sediments.”

49 *We clarified that guidelines are primarily provided to aid sample analysis of soil*
50 *and sediment samples prone to volcanic glass inputs. However, we would like to*
51 *emphasize that one can easily see methodological advantages and application*
52 *possibilities of the described approach (using Si:Al in combination with alkaline*
53 *reactivity constants) to tackle contributions of other non-biogenic sources, such as*
54 *clays and nanocrystalline fractions. This is also suggested in section 4.2.2 and 4.3.1,*
55 *but we do agree that the absence of mineralogical information limits the generality*
56 *of our interpretation regarding the contribution of other than volcanic non-*
57 *biogenic fractions. We therefore refer to an extensive line of research performed by*
58 *our co-author L. Barão (Barão et al., 2014. EJSS; Barão et al., 2015. LOM; Barão,*
59 *2015, thesis) who exemplifies the usefulness of the method for such cases.*

60

61 C3: Rephrased p17 line 534 dealing with limited knowledge of mineralogical
62 composition samples.

63 *Rephrased*

64

65 C4: The reactivity constant is not a standard, provide more detail on the
66 rationale of its use.

67 *Included in the methodology section 2.3.2*

68

69 C5: Don't abbreviate MDS and provide unit.

70 *Changed throughout the manuscript*

71

72 C6: Would it be possible to define a very pure tephra sample as a standard?

73 *Due to the large variation in the chemical composition of pure glass shards, as*
74 *shown on the TAS diagram, it is difficult to use one standard with fixed dissolution*
75 *parameters. However, we provide a clear framework based on their intrinsic Si:Al*
76 *ratio (defined with EMPA) and dissolution characteristics to interpret the*
77 *dissolution parameters of pure glass shards. Additionally, the heavy liquid*
78 *separation was indeed performed to isolate glass shards from clays,*
79 *nanocrystalline minerals and biogenic Si fractions, and to validate our proposed*
80 *"typical" dissolution pattern obtained for fresh deposits (defined group 1 in the*
81 *manuscript) depleted of such fractions. However, pre-treatment steps hampered*
82 *straightforward interpretation.*

83

84 C7: *We agree that pretreatment need to be conducted with care, and suggest*
85 *additional research focusing on delineating the exact effects and consequences for*
86 *BSi determination.*

87

88 C8: Fig 1, provide more info on TAS?

89 *Additional information is provided in the figures captions. TAS is a standard way of*
90 *classifying pyroclastic volcanic rocks based on non-genetic features, and commonly*
91 *applied to classify tephra samples.*

92

93 **Additional changes based on the editor's suggestions:**

94

95 C9: Alkaline extraction techniques are not the only used method to determine
96 BSi.

97 *We have included an overview of alternative methods.*

98
99 C10: Presentation of results according to their origin (i.e. soil, peat or lake
100 sediment). Do deposits represent the extreme in terms of percentage tephra in
101 the samples.
102 *We disagree as samples at the moment are ordered following a decreasing*
103 *contribution of tephra, and increasing complexity of the samples composition. This*
104 *corresponds with the observed patterns in dissolution properties and therefore*
105 *makes it clearer for the reader to interpret the classification in three groups.*
106
107 C11 Clarify to what extent heavy liquid separation aided this study?
108 *Heavy liquid separation is used to obtain more 'pure' shard and diatom signatures*
109 *for our more complex samples. These purified samples are used to validate the*
110 *fraction modeling results of the continuous extraction. Our results indicate that*
111 *purification was successful (single fraction left; section 3.2.2), but chemical pre-*
112 *treatment during heavy liquid separation altered the dissolution properties. The*
113 *heavy liquid separation does not provide additional quantitative information*
114 *regarding the influence of tephra material on determinations of biogenic silica. As*
115 *suggested, we have removed all such references. A good suggestion is made to*
116 *construct an artificial sample series made of pure glass shard mixtures and BSi to*
117 *optimize the suggested correction method (section 4.2.3). However one should be*
118 *careful with chemical pre-treatment techniques as outlined in the manuscript.*
119
120 C12: Improve the presentation of the results.
121 *We clarified the presentation of the results. The factor 2-5 compares 3-5h Na₂CO₃*
122 *and NaOH, not 20-24h Na₂CO₃ and NaOH. However, we indicated that also there*
123 *we observe extreme differences (>10) for which we do not have a clear explanation.*
124
125 C13: How might grain size influence the dissolution curves?
126 *The method assumes complete dissolution of the biogenic Si fraction, this means*
127 *Si_{Alk} should be independent of grain size. However, our data indicates that for other*
128 *contributors like volcanic glass incomplete dissolution leads to an apparent*
129 *contribution to Si_{Alk} measurements. Such partial dissolution depends on the*
130 *reactive surface area, and therefore grain size. This probably partially explains the*
131 *variation in k-factor for the slower fraction. It is, however, unlikely that grain size*
132 *explains the whole range of dissolution parameters observed. Artificially reducing*
133 *the grain size is likely to affect the contribution of non-biogenic Si_{Alk} as grinding*
134 *will enhance available reactive surface area. This needs to be avoided to exclude*
135 *experimentally induced bias on the BSi estimate despite the probably improved*
136 *comparability of the dissolution curves.*
137
138 C14: Where does the Vedde Ash fit in?
139 *Indeed, its weathered character (most probably of the basaltic component) led to*
140 *the contribution of other non-biogenic Si fractions assumed to be the*
141 *nanocrystalline weathering products (see figure 2, 3 and 5 for classification and*
142 *section 4.2.3 for explanation).*
143
144 C15: What is the detection limit of the alkaline extraction and what is the
145 analytical uncertainty?

146 *Detection limit depends on the method used, but for alkaline extraction values of*
147 *0.01 wt% SiO₂ are usually assumed to be the lower level of accuracy (i.e. soil*
148 *studies). As shown in Table 2, the analytical uncertainty for tephra samples exceeds*
149 *the detection limit. The within lab analytical uncertainty for pure biogenic samples*
150 *and non-volcanic soil samples are normally very low (from negligible to 10%,*
151 *Conley, 1998), but increase with the contribution of clays (see section 4.2.3 and also*
152 *Barão et al. 2015. LOM). The incomplete dissolution after 3-5 hours in Na₂CO₃*
153 *probably explains the “higher” relative analytical uncertainty for our samples, and*
154 *why they seem to decrease for the 20-24h set. For NaOH, the consistent agreement*
155 *between measured alkaline extracted Si:Al ratios for shards and those based on the*
156 *EMPA suggests accurate estimates. However we highlight the necessity to conduct*
157 *an elaborate uncertainty analysis on the parameterization of the curve modeling in*
158 *the concluding section.*

159

160 C16: Correct value cited for Prokopenko et al.

161 *Corrected*

162

163 C17: The study was not really designed to infer implications for downcore
164 variations in BSi content for paleorecords, or to detect the potential indirect
165 effect of tephra deposition on diatom community and productivity in lakes.

166 *We only partly agree with this comment. We understand the concern that our study*
167 *design only allows to infer conclusions based on direct quantifiable effect of*
168 *volcanic shard contribution, i.e. reconnaissance and significant contribution during*
169 *alkaline extraction. We therefore reformulated (acknowledging previous*
170 *recommendations) and reduced the discussion part concerning the indirect effect*
171 *that tephra deposition might have on the diatom signature of lakes.*

172 *We acknowledge that more studies are required to confirm the significance of the*
173 *downcore effect of tephra contributions to BSi measurements in oligotrophic*
174 *systems (the most sensitive systems). However, we believe that a simple comparison*
175 *of the absolute contribution of volcanic shard and its weathering products with*
176 *interpretable shifts in observed downcore variation in BSi gives already a clear*
177 *indication of its potential consequences (first two paragraphs of section 4.3.2).*
178 *Additionally, we would like to stress that although many authors have suggested*
179 *this relationship; all have failed to quantify its effect. Therefore, we believe that our*
180 *methodologically focused study provides new insights to what extent tephra*
181 *deposition affects the interpretation of BSi records in paleo records. We believe this*
182 *justifies the inclusion of section 4.3.2 in its reduced format in the final manuscript,*
183 *and additionally included suggestions for future research to strengthen our*
184 *findings.*

185

186 Fig. 1 & Table 1 were updated, Fogo A is classified as a trachyte instead of dacite.

187

188 References:

189 **Phd thesis: Lúcia Barão, 2015, Biogenic and non-biogenic Si pools in terrestrial*
190 *ecosystems: results from a novel analysis method, University of Antwerp, Antwerp*

191 **Conley, D.: An interlaboratory comparison for the measurement of biogenic silica*
192 *in sediments, MARINE CHEMISTRY, 63, 39-48, 1998.*

193 **Derry, L., Kurtz, A., Ziegler, K., and Chadwick, O.: Biological control of terrestrial*
194 *silica cycling and export fluxes to watersheds, NATURE, 433, 728-731, 2005.*

195 *Meunier, J. D., Kirman, S., Strasberg, D., Nicolini, E., Delcher, E., and Keller, C.: The
196 output and bio-cycling of Si in a tropical rain forest developed on young basalt
197 flows (La Reunion Island), *GEODERMA*, 159, 431-439, 2010.

198 **The contribution of tephra constituents during biogenic silica**
199 **determination: implications for soil and paleoecological studies**

200
201 Wim Clymans^{1,*}, Lúcia Barão², Nathalie Van der Putten¹, Stefan Wastegård³,
202 Guðrún Gísladóttir⁴, Svante Björck¹, Bertrand Moine⁵, Eric Struyf² and Daniel J.
203 Conley¹

204
205 ¹Department of Geology, Lund University, Sölvegatan 12, SE-22362 Lund,
206 Sweden

207 ²Department of Biology, Ecosystem Management, University of Antwerp,
208 Universiteitsplein 1, BE-2610 Wilrijk, Belgium

209 ³Department of Physical Geography, Stockholm University, SE-10691 Stockholm,
210 Sweden

211 | ⁴Institute of **Life and Environmental Sciences**, and the Nordic Volcanological
212 Center, University of Iceland, Sturlugata 7, IS-101 Reykjavík, Iceland

213 ⁵Université de Lyon, Magmas et Volcans (UBP-UJM-CNRS-IRD), 23 rue Dr. P.
214 | Michelin, F-42023 Saint-Etienne, France

215
216 *Corresponding author. Tel.: +46-4622-27888; fax: +46-4622-24830
217 *E-mail address:* wim.clymans@geol.lu.se

218

219 **Abstract**

220 Biogenic silica (BSi) is used as a proxy by soil scientists to identify biological
221 effects on the Si cycle and by paleoecologists to study environmental changes.

222 Alkaline extractions are typically used to measure BSi in both terrestrial and
223 aquatic environments. The dissolution properties of volcanic glass in tephra
224 deposits and their nano-crystalline weathering products are hypothesized to
225 overlap those of BSi, however, data to support this behavior are lacking. The

226 | potential that Si-bearing fractions dissolve in alkaline media (Si_{Alk}) that do not
227 necessarily correspond to BSi, question the applicability of BSi as a proxy. Here,

228 analysis of 15 samples reported as tephra-containing allows us to reject the
229 hypothesis that tephra constituents produce an identical dissolution signal to

230 that of BSi during alkaline extraction. We found that dissolution of volcanic glass
231 shards is incomplete during alkaline dissolution. Simultaneous measurement of

232 Al and Si used here during alkaline dissolution provides an important parameter
233 to enable us to separate glass shard dissolution from dissolution of BSi and other

234 Si-bearing fractions. The contribution from volcanic glass shard (between 0.2-4
235 wt% SiO_2), the main constituent of distal tephra, during alkaline dissolution can

236 be substantial depending on the total Si_{Alk} . Hence, soils and lake sediments with
237 low BSi concentrations are highly sensitive to the additional dissolution from

Wim Clymans 8/5/2015 15:33

Deleted: Department of Geography and
Tourism,

Wim Clymans 8/5/2015 15:34

Deleted: Earth Sciences

Wim Clymans 24/2/2015 08:58

Deleted: Just in time

Daniel Conley 21/5/2015 06:56

Deleted: understanding

Daniel Conley 21/5/2015 06:56

Deleted: the

Daniel Conley 21/5/2015 06:56

Deleted: that

245 tephra constituents and its weathering products. We advise evaluation of the
246 potential for volcanic or other non-biogenic contributions for all types of studies
247 using BSi as an environmental proxy.

248 **Keywords: Biogenic silica, Tephra, Alkaline extraction, Paleoecology,**
249 **Silicon cycle, Volcanic glass**

250 **1 Introduction**

251

252 Many plant and algae species take up dissolved silica (DSi) from the environment
253 and produce biogenic silica (BSi), a hydrated, amorphous SiO₂ polymorph that
254 provides structural and physiological benefits (Guntzer et al., 2012). BSi is
255 regularly estimated by soil scientists or paleoecologists using various alkaline
256 extraction techniques. These extraction techniques have supplanted other
257 methods in general usage, including microfossil counts (Leinen et al., 1985),
258 infrared spectroscopy (Meyer-Jacob et al., 2014) and X-ray diffraction. Each
259 technique has specific benefits and limitations (Ohlendurf and Storm, 2008). The
260 alkaline extraction techniques are applied to a range of environments and
261 archives, including soils, peat deposits, lake and marine sediments, wetland and
262 floodplain deposits and suspended matter in rivers (Andresen et al., 2004;
263 Clymans et al., 2011a; Clymans et al., 2011b; Cornelis et al., 2010; Fernández et
264 al., 2013; Frings et al., 2014b; Verschuren et al., 2002). In terrestrial ecosystems
265 vegetation may buffer DSi delivery to streams and rivers (Churchman and Lowe,
266 2012; Struyf and Conley, 2012). Hence, the magnitude of BSi accumulation in
267 soils is a key component in the biological buffering capacity of the Si cycle in an
268 ecosystem. Paleoecologists use BSi as a proxy for diatom productivity, and apply
269 this to infer changes in e.g. nutrient availability (Conley et al., 1993; Heathcote et
270 al., 2014), hydrology (Andresen et al., 2004), atmospheric circulation (Harper et
271 al., 1986; Johnson et al., 2011; Verschuren et al., 2002) and temperature (Adams
272 and Finkelstein, 2010; Prokopenko et al., 2006).

273

274 The methods vary in detail but all assume a difference in dissolution rate that
275 forms the basis of the separation of Si from mineral silicates and amorphous

Wim Clymans 4/5/2015 14:20

Deleted: se

Wim Clymans 4/5/2015 14:16

Deleted:

278 biological fractions. Within the range of alkaline solutions used in the
279 experiments a fraction of the material may release Si at a slow and apparently
280 constant rate over the duration of the extraction (from here on referred to as a
281 'linearly dissolving fraction'). This corresponds to dissolution of mineral silicates
282 (Conley and Schelske, 2001; Koning et al., 2002). Some fractions may rapidly
283 release some or all of their Si within the duration of the extraction (from here on
284 'non-linearly dissolving fractions') and this non-linear fraction is conventionally
285 interpreted as the BSi fraction (DeMaster, 1981).

286

287 Unfortunately, various non-BSi fractions also release Si either completely or
288 partly in a non-linear manner in alkaline media, questioning the interpretation of
289 the non-linear part as biological in origin (Cornelis et al., 2011a; Gehlen and van
290 Raaphorst, 1993; Koning et al., 2002). Cornelis et al. (2011b) reviewed sources
291 that may completely dissolve and find that in addition to biogenic remains (e.g.
292 phytoliths, diatoms), inorganic forms such as Al-Si precipitates, volcanic glass
293 shards, adsorbed Si on amorphous Fe-oxides and nanocrystalline fractions such
294 as allophanes and imogolite, can comprise a substantial portion of the non-
295 linearly dissolving Si. Partial dissolution of clays can also rapidly release Si
296 (Barão et al., 2015; Koning et al., 2002). We introduce a procedural term ' Si_{Alk} '
297 (alkaline extracted Si) to refer to the full range of Si-bearing phases that dissolve
298 non-linearly under normal experimental conditions. It is becoming apparent that
299 Si_{Alk} does not necessarily correspond only to the BSi fraction, and thus caution is
300 warranted due to its implications for interpretation of the putative BSi record in
301 both soil and paleoecological studies.

302

303 Several studies have suggested that glass shards and their weathering products
304 (e.g. nanocrystalline minerals and secondary clays) could affect Si_{Alk}
305 measurements, as their dissolution characteristics in alkaline solutions can
306 overlap with the biogenic fraction (Barão et al., 2015; Hashimoto and Jackson,
307 1958; Sauer et al., 2006). Discrete volcanic ash deposits, composed of shards,
308 minerals together with pumice and rock fragments, known as tephra are
309 common in sedimentary archives; indeed, they form the basis of
310 tephrochronology (e.g. Lowe, 2011), a powerful technique for establishing age-

311 equivalence between sites. If dissolving glass (or mineral grain) in a tephra
312 releases Si in a similar way to BSi during dissolution in alkaline solutions, it has
313 the potential to make interpretation of Si_{Alk} difficult, since a change will not
314 uniquely represent a change in environmental conditions but also perhaps
315 periods of volcanic activity. Additionally, because of their often rapid dissolution,
316 glass, pumice, and other constituents in tephra can potentially induce elevated
317 DSi concentrations in lakes, causing shifts in phytoplankton communities (Lotter
318 et al., 1995; Hickman and Reasoner, 1994). Such a shift in the sedimentary
319 record may be incorrectly ascribed to a change in environmental conditions
320 providing a secondary indirect pathway to biased interpretations.

321

322 Here, we investigate volcanic glass shards and their weathering products as a
323 confounding factor during Si_{Alk} determination. We tested 1) dissolution
324 characteristics of glass in tephra deposits, and 2) whether tephra-derived
325 constituents contribute to Si_{Alk} measurements during alkaline extraction, and 3)
326 how such contributions affect the Si_{Alk} measurements in soils, sediments and
327 peats. We find that glass shards do not produce an identical dissolution signal to
328 that of BSi during alkaline extractions. However, the contribution of glass shards
329 to BSi can be substantial when low BSi concentrations are encountered in
330 environmental archives with important repercussions for soil and
331 paleoecological studies.

332 **2 Materials & Methods**

333 **2.1 Tephra Samples**

334 Fifteen samples reported as tephra-containing and covering a representative
335 range of chemical composition (basaltic to rhyolitic), eruption dates (from 2010
336 AD until 48 ka BP), geographical provenance (northern and southern latitudes)
337 and environments (fresh deposits, soils, lakes and peat archives) have been
338 retrieved from archived samples (Table 1; Fig. 1). We used tephra collections
339 from tephra deposits described previously in soil and paleoecological studies
340 representing a gradient in weathering state.

341 **Table 1**

342 **2.2 Sample Treatment**

343 All samples were split in two parts to develop two distinct sample sets:
344 untreated *versus* treated. Untreated samples were immediately subjected to
345 alkaline extraction (section 2.3). The goal of treating samples is to isolate
346 relatively pure biogenic and volcanic glass derived fractions, which will allow us
347 to evaluate the robustness of the inferences made from the dissolution of the
348 untreated samples. Samples were subjected to standard pre-treatment and
349 heavy-liquid separation, described below, with additional magnetic separation
350 or sieving steps where necessary (Mackie et al., 2002; Morley et al., 2004;
351 Turney, 1998).

352 **Figure 1**

353 **2.2.1 Pre-treatment**

354 A 0.5-1 g subsample was weighed into a 15 ml centrifuge tube to which 30%
355 hydrogen peroxide (H₂O₂) was repeatedly added to remove organic matter at
356 80°C until reaction cessation. One millilitre of 10% HCl solution was added to
357 disaggregate the material and dissolve any soluble inorganics (e.g. carbonates)
358 and left until the reaction ceased. After each treatment step, the sample was
359 washed three times in deionized water (MilliQ).

360 **2.2.2 Heavy-liquid separation**

361 Heavy liquid separation is used to obtain concentrated siliceous organism
362 samples (i.e. diatoms and sponges) (Morley et al., 2004) and concentrated glass
363 shard samples (e.g. Turney, 1998). The biogenic part is concentrated by
364 centrifuging in sodium polytungstate (SPT) having a relative density of 2.3 g cm⁻³.
365 Prior to each centrifuge step, samples were thoroughly mixed, and if necessary
366 placed in an ultrasonic bath to disaggregate the material. The floating material (<
367 2.3 g cm⁻³) was dried (70°C) and assessed with SEM for purity, i.e. biogenic
368 material, or possible contamination from pumice and other non-biogenic light
369 fractions. The residue (>2.3 g cm⁻³) was centrifuged in SPT at a relative density of
370 2.5 g cm⁻³. Both floating material (between 2.3 g cm⁻³ and 2.5 g cm⁻³) and residue
371 (>2.6 g cm⁻³) were washed with MilliQ. The latter should contain heavy minerals,
372 and only a limited amount of glass shards, which should instead be concentrated

373 within the 2.3 to 2.5 g cm⁻³ bracket. All residues were microscopically checked
374 for their purity.

375

376 The separation only rarely resulted in high-purity end-products. Additional *ad*
377 *hoc* sample specific treatments were conducted to improve the separation. In
378 case of high concentration of low-density shards (e.g. pumice) within the
379 biogenic sample (<2.3 g cm⁻³), a wet-sieving step was used to separate the
380 biogenic siliceous bodies from shards. Size-distributions for each fraction were
381 determined using light microscopy (Nikon SMZ1500, x16) and the NIS-Elements
382 software for size measurements. The selected mesh size corresponded with the
383 point of minimum overlap. In case of basaltic tephra shards (i.e. > 2.7 g cm⁻³)
384 magnetic separation of the >2.6 g cm⁻³ (Mackie et al., 2002) was applied to
385 concentrate pure basaltic shards.

386 **2.3 Alkaline extraction techniques**

387 Two different alkaline extractions were used to determine the Si_{Alk} content and
388 dissolution characteristics of the untreated and the isolated tephra and biogenic
389 silica fractions of the treated samples: the sequential 0.1 M Na₂CO₃ and the
390 continuous 0.5 M NaOH method.

391 **2.3.1 Sequential wet-alkaline extraction method: 0.1 M Na₂CO₃**

392 The Na₂CO₃ extraction is a weak-base method developed by DeMaster (1981)
393 who described that while alumino-silicates release Si linearly over time, most BSi
394 dissolves completely within the first 2 hrs of the digestion. In our analysis
395 (Conley and Schelske, 2001), approximately 30 mg of dried sample (< 2 mm) was
396 mixed in 40 ml of 0.1 M Na₂CO₃ solution and digested for 5 hours at 85°C. A 0.5
397 ml aliquot was removed after 3, 4 and 5 hours and neutralized with 4.5 ml of
398 0.021 M HCl, before DSi determination by the automated molybdate-blue
399 method (Grasshoff et al., 1983) using a Smartchem 200 (AMS Systea) discrete
400 analyser. The Si_{Alk} was calculated by determining the intercept of the regression
401 between total extracted Si and extraction time. Extrapolating the Si release to the
402 intercept is assumed to correct for mineral dissolution of Si. To evaluate its
403 suitability to correct for mineral dissolution, the typical subsampling scheme
404 was prolonged to 24 hrs and additional 0.5 ml subsamples were taken at 9, 10

405 and 11 hrs and again at 20, 22 and 24 hrs, and diluted in 9.5 ml 0.010 M HCl
406 instead of 4.5 ml to obtain optimal dilution.

407 **2.3.2 Continuous extraction method: 0.5 M NaOH**

408 We applied a stronger NaOH (0.5 M) digestion protocol (Barão et al., 2014;
409 Koning et al., 2002) with continuous monitoring of the extracted Si and
410 aluminium (Al) concentration through time. Briefly, between 20 and 100 mg of a
411 sample was mixed with 180 ml of 0.5 M NaOH (pH = 13.7) in a stainless steel
412 vessel. The vessel was incubated in a water bath at a constant temperature of
413 85°C and continuously stirred with a rotor to obtain a homogeneous mixture.
414 The vessel was sealed to prevent evaporation. The extraction fluid was fed into a
415 Skalar continuous flow analyzer at 0.42 ml min⁻¹. Si and Al concentrations were
416 determined simultaneously using the spectrophotometric molybdate-blue
417 method for Si (Grasshoff et al., 1983) and lumogallion fluorescence for Al (Hydes
418 and Liss, 1976) for 30-40 minutes.

419 A simultaneous fit of dissolved Si and Al curves was performed using equation
420 (1).

421

$$422 \quad Si_t = \left(\sum_{x=1}^n Si_{Alk,x} \times (1 - e^{-k_x \times t}) \right) + b \times t \quad Al_t = \left(\sum_{x=1}^n \frac{Si_{Alk,x}}{Si:Al_x} \times (1 - e^{-k_x \times t}) \right) +$$
$$423 \quad \frac{b \times t}{Si:Al_{min}} \quad (1)$$

424

425 where Si_t and Al_t is the pool of extracted silica and aluminum at time t ($\mu\text{mol l}^{-1}$);
426 $Si_{Alk,x}$ is the total pool of Si_{Alk} ($\mu\text{mol l}^{-1}$) of fraction x ; k is a parameter that reflects
427 the non-linear reactivity of the sample (min^{-1}); b reflects the linear reactivity and
428 $Si:Al_x$ and $Si:Al_{min}$ represent their respective Si:Al ratios. The dissolution curves
429 of Si and Al were used to identify fractions based on their Si:Al ratios. This
430 principle was first applied by Koning et al. (2002) in marine sediment samples,
431 where almost all alkaline extracted Si has a biogenic source, overprinted by a low
432 $Si:Al_x$ component from clay minerals dissolution. They showed that some
433 fractions that would be considered as biogenic using linear phase extrapolation
434 (i.e. the sequential extraction, above) were actually clay contamination, based on
435 the low $Si:Al_x$ ratios (between 1 and 4) in these fractions. We hypothesize that
436 glass from tephra will resemble such behaviour because of their relatively high

437 Al content. The k-parameter reflects how fast a Si bearing fraction reaches
438 complete dissolution in an alkaline media, and depends on bonding strengths
439 and specific reactive surface areas. Here, relative differences of k-values between
440 modelled fractions are used to classify high and low reactive fractions in alkaline
441 media, where nanocrystalline and absorbed Si fractions are suggested to be
442 more rapidly released as compared to biogenic Si fractions (Barão et al., 2015).

Stefan 19/5/2015 16:40

Deleted: y

444 The number of fractions (x) in the first order model was determined by
445 consecutively allowing an extra fraction to obtain an optimal model fit (i.e.
446 reducing the RMSE using the Solver function within Microsoft Excel).

447 3 Results

448 3.1 Sequential wet-alkaline extraction method – 0.1 M Na₂CO₃

449 Table 2

450 Alkaline silica (Si_{Alk}) extracted from a total of 14 tephra-containing samples
451 (EFJ2010_1504 not included) based on the 3-5h mineral dissolution slope (wt%
452 SiO₂ h⁻¹) vary between 0.3 and 16.7 wt% SiO₂ with an average of 3.01 ± 3.91 wt%
453 SiO₂. Mineral dissolution slope ranges between 0.03 and 0.65 wt% SiO₂ h⁻¹ with
454 an average of 0.35 ± 0.21 wt% SiO₂ h⁻¹. This high standard deviation suggests
455 variability within samples, but is heavily influenced by two outliers (Reclus R1
456 and Tuhua tephra); median Si_{Alk} and mineral dissolution slope are 1.56 wt% SiO₂
457 and 0.28 wt% SiO₂ h⁻¹, respectively.

Wim Clymans 4/5/2015 11:42

Formatted: Subscript

Wim Clymans 4/5/2015 11:41

Deleted: (MDS)

Wim Clymans 4/5/2015 11:42

Formatted: Superscript

Wim Clymans 4/5/2015 11:43

Deleted: MDS

Wim Clymans 4/5/2015 11:43

Deleted: MDS

458
459 The median Si_{Alk} using the 20-24h mineral dissolution slope was 3.63 wt% SiO₂
460 with a median slope of 0.12 wt% SiO₂ h⁻¹. A paired t-test (signed rank) showed
461 that both (corrected) Si_{Alk} concentrations and mineral dissolution slope differed
462 significantly between the 3-5hrs and the 20-24hrs sampling intervals.

Wim Clymans 4/5/2015 11:44

Deleted: MDS

Wim Clymans 4/5/2015 11:44

Deleted: MDS

463
464 There is a large variability in the shape of the curves in extracted Si through time
465 (Fig. 2). Some samples exhibit a continuously gently decreasing slope with time
466 (Fig. 2.a), while others show initial rapid dissolution followed by a steep linear
467 increase (Fig. 2.b), whereas others increase rapidly but are followed by no

474 increase or only a minimal increase in Si extracted with time (Fig. 2.c).
475 Numerically, we define this gradient through comparing the Si_{Alk} after 3-5hrs
476 with those obtained after 20-24hrs (Table 2): we observe respectively high (3.0-
477 7.1), medium (1.5-2.5) and low (1-1.8) ratios. Ideally, constant mineral
478 dissolution with no additional amorphous Si extracted after 3hrs would
479 correspond to a ratio of 1.

480 **Figure 2 & Figure 3**

481 **3.2 Continuous alkaline extraction method: 0.5 M NaOH**

482 **3.2.1 Curve decomposition**

483 Results of curve fitting the continuous monitored Si and Al data during the
484 extractions are presented in Table 3 and Figures 2 and 3. Si_{Alk} concentrations
485 vary between 0.27 and 23.4 wt% SiO_2 with an average of 4.54 ± 6.08 wt% SiO_2
486 and a median of 2.31 wt% SiO_2 . On average, but not always, these concentrations
487 are significantly higher than those measured during the Na_2CO_3 3-5 h extraction
488 (section 3.1; $p=0.0016$), but do not differ significantly with the Na_2CO_3 20-24 h
489 extraction ($p=0.1540$; non-parametric t-test). However, relative differences
490 between the NaOH and Na_2CO_3 3-5 h extraction, can be up to factor 2-5, and
491 values tend to be lower (up to 10 times) than those measured during the Na_2CO_3
492 20-24 h extraction.

493
494 The shape of the dissolution curves suggests the presence of three distinct
495 dissolution patterns similar to using the Na_2CO_3 methodology. A first set of
496 curves show a gently decreasing slope with time, and limited contribution of Al
497 (Fig. 2d – Group 1). The second set of curves shows a rapid increase at the onset
498 for both Si and Al, and afterwards evolves towards a more linear increase (Fig. 2e
499 – Group 2). The final set is characterized by a rapid increase at the onset with
500 varying contributions of Al, but mostly an order of magnitude lower than
501 extracted Si concentrations with a near zero or high mineral dissolution slope
502 (Fig. 2f – Group 3).

503
504 Optimal fits of the model to predict the dissolution curve included between one
505 to three different Si_{Alk} fractions each with a specific k-parameter and Si to Al

Wim Clymans 4/5/2015 15:21

Deleted: These values

Wim Clymans 4/5/2015 15:34

Formatted: Subscript

Wim Clymans 4/5/2015 15:34

Deleted: two values

Wim Clymans 4/5/2015 15:26

Deleted: 5

Wim Clymans 4/5/2015 15:34

Formatted: Subscript

509 ratio (Table 3). We used the number of non-linear fractions (first order - see
510 equation 1) and their Si:Al_x to group the samples (see discussion, Fig. 2d-f, and
511 Table 3). One group of samples exhibited one non-linear fraction that was
512 released slowly with a k between 0.05 and 0.5 min⁻¹. The linear dissolution is
513 responsible for the majority of the increase in Si and Al concentrations through
514 time. Si:Al_x ratios for both fractions are approximately equal and range between
515 3 and 5.

516

517 **Table 3**

518

519 A second group has two fractions that dissolve non-linearly. The non-linear
520 fractions evolve rapid (k>0.7 min⁻¹) and slow (k<0.5 min⁻¹), respectively,
521 towards complete dissolution. The Si:Al_x ratio of the slow fraction falls between 1
522 and 2.5. The rapid reaction releases typically more Al leading to low Si:Al
523 (< 1). The Si:Al_{min} ratio of the linear fraction ranges between 1 and 3.5. Finally,
524 two fractions that dissolve non-linearly typify a third set of samples: a rapid (k >
525 0.7 min⁻¹) fraction with Si:Al_x mostly below 1 and a slow fraction (k < 0.5 min⁻¹)
526 with Si:Al_x above 8. One exception (Reclus R₁) has three fractions but no mineral
527 fraction and differs by having two slow fractions instead of one.

528 **3.2.2 Validation of curve decomposition procedure**

529 Dissolution curves using 0.5 M NaOH for all concentrated shard samples
530 (rhyolitic: between 2.3 g cm⁻³ to 2.5 g cm⁻³; basaltic > 2.5 g cm⁻³) were best
531 approximated with a single non-linear fraction and a linear (i.e. mineral) fraction
532 indicating successful physical separation of shards (see Table 4). Mineral
533 dissolution contributions were typically large in total Si and Al release, being the
534 main source after on average 5 minutes of dissolution for Al release. The initial Si
535 and Al release appears to be faster than before the cleaning and separation
536 treatment. This is reflected in higher Si:Al_x ratios and k-values. One exception -
537 the Reclus R₁ sample - did not contain a retrievable amount of shards.

538

539 The BSi rich samples (< 2.3 g cm⁻³) were fitted with a single non-linear fraction in
540 absence of a linear fraction. The only exception is the Tuhua tephra where two

541 non-linear fractions with varying dissolution rate were fitted: defined as a rapid
542 (0.47) and slow (0.05) k. All Si:Al_x were higher than 100. The total extracted Si
543 content averaged on 72 ± 11 wt% SiO₂.

544

545 **Table 4**

546 **4 Discussion**

547 Earlier studies have hypothesized that volcanic glass shards substantially
548 contribute to measured Si_{Alk} (Cornelis et al., 2011b; Lyle and Lyle, 2002; Sauer et
549 al., 2006). In the following, we discuss the specific dissolution characteristics of
550 glass shards, during alkaline extraction and implications for soil and
551 paleoecological studies. We formulate guidelines for the use of alkaline
552 extraction techniques to determine BSi in soils and sediments [prone to volcanic](#)
553 [glass inputs](#).

554 **4.1 Incomplete dissolution during digestion**

555 In theory, Si_{Alk} should be insensitive to the choice of aliquot times during Na₂CO₃
556 extraction, if the dissolution of minerals [does](#) not violate the two key
557 assumptions of the original protocol outlined by DeMaster (1981): (i) complete
558 dissolution of all Si_{Alk} fractions within three hours, and (ii) the mineral fraction
559 should exhibit linear behavior during the course of the dissolution experiment.
560 The linear behavior is assumed to be caused by minimal changes in reactive
561 surface area of crystalline minerals during dissolution in a weak base, e.g. 0.1 M
562 Na₂CO₃.

563 Higher Si_{Alk} concentrations (Table 2) and lower [mineral dissolution slope](#) values
564 after 20-24 h for our samples suggest a prolonged non-linear behavior. We
565 interpret this as evidence for incomplete dissolution of alkali extractable
566 fractions within the first 3 h of extraction. Complete dissolution of glass takes
567 considerably longer than 3 h causing Si_{Alk} to be underestimated when sub-
568 sampling only over the 3-5 h time period. In addition, a decrease in reactivity
569 during the 24 h extraction violates the second assumption. Our samples must
570 contain another fraction that violates the second assumption, and only reaches a

Wim Clymans 4/5/2015 11:44

Deleted: MDS

572 state of apparent linear dissolution after the 5 hour sampling.

573 We observe a gradient in the severity (high degree, medium degree and low
574 degree) of incomplete dissolution expressed as the deviation from an ideal Si_{Alk}
575 (22-24 h/3-5 h) ratio of 1. Samples were grouped according to their extent of
576 deviation from the ideal. Most samples are not newly formed pure volcanic
577 deposits but instead are a complex set of samples from lakes, soils and peat bogs
578 (Table 1). We suggest that the differences in the extent of dissolution and in their
579 dissolution curves represent variations in composition and abundance of
580 different Si_{Alk} sources. Unfortunately, the Na_2CO_3 method cannot define the
581 origin of the different Si_{Alk} fractions. This makes quantification of the
582 contribution of volcanic material to BSi impossible.

583

584 **4.2 Towards separation of the different fractions**

585 The use of Si:Al ratios using the continuous NaOH extraction methodology can
586 improve the interpretation of dissolution and uncertainty of the Si source (Barão
587 et al., 2014). NaOH should also be more efficient in dissolving all amorphous and
588 nanocrystalline material present (Müller and Schneider, 1993; Gehlen and van
589 Raaphorst, 1993). We combine dissolution parameters in NaOH with microscopy
590 to attribute specific dissolving or releasing fractions to our three defined groups
591 (see section 3.2.1 and Fig. 3).

592 **4.2.1 A shard signature**

593 Group 1 represents relatively pure tephra samples (Fig. 2a, d) where dissolution
594 of glass shards dominates. Our data suggests that glass shards release the
595 majority of Si and Al at a rapid and a constant rate during the time period (ca. 30
596 min) we monitor dissolution in NaOH. In contrast to Na_2CO_3 , the stronger NaOH
597 seems to obtain apparent linear dissolution within the course of the experiment,
598 after an initial non-linear release. This initial decrease in reactivity followed by a
599 substantial constant Si and Al release corroborates previous observations
600 describing the stoichiometric dissolution of glass shards (Oelkers and Gislason,
601 2001; Stephens and Hering, 2004). Si:Al ratios of the non-linear Si_{Alk} and linear
602 fraction coincide with Si:Al ratios from unweathered glass shards ($\text{Si:Al}_{\text{Solid}}$). Si:Al

603 ratios of the pure tephra samples (presumably mainly glass) are plotted along
604 the 1:1 line demonstrating stoichiometric behavior (Fig. 4a).

605

606 Oelkers and Gislason (2001) delivered a theoretical framework for volcanic
607 glass shard dissolution at acidic and alkaline conditions that adequately
608 describes our observed dissolution patterns in both Na_2CO_3 and NaOH solutions.
609 Initially, proton exchange reactions will lead to the removal of univalent and
610 divalent cations from the shard surfaces, followed by a partial removal of Al from
611 the framework through the same process. Finally, Si liberation is possible
612 through the weakened state of Si as it is present in Si tetrahedrals, i.e. only
613 partially attached to the framework by only one or two bridging oxygen atoms
614 primarily located at the edges and tips of the shard. As smoothening of the
615 shards progresses, and depending on the abundance of hydrated sites, the
616 weakened state of Si at the edges can lead to faster release of Si at the onset,
617 which decreases as the edges become rounded. The rounding of edges is
618 responsible for the observed Si_{Alk} content when glass shards are dissolved.
619 Afterwards, glass shards will continue to release Si and Al at a steady
620 stoichiometric rate (see also Hodder et al., 1990). Hence, the dissolution pattern
621 reflects the continuous but incomplete dissolution of glass shards. This process
622 makes the dissolution of glass shards distinct from the dissolution of other non-
623 biogenic (e.g. nanocrystalline minerals) or biogenic fractions and adsorbed Si
624 and Al release. These processes occur rapidly at the onset of NaOH extraction but
625 do not lead to a fast constant release after unspecified time (Barão et al., 2014;
626 Hashimoto and Jackson, 1958).

627

628 Based on the pure samples of tephra (i.e. glass rich), we suggest that shards have
629 a distinct dissolution signature discernable using continuous monitoring during
630 a 0.5 M NaOH extraction. The three defining characteristics are: 1) the mineral
631 dissolution slope is extremely high ($0.028\text{-}0.120 \text{ wt}\% \text{ SiO}_2 \text{ min}^{-1}$) with 2) a Si:Al
632 ratio in the extracted aqueous phase between 3 and 5 equal to that of un-
633 weathered shards confirming stoichiometric dissolution and its volcanic origin,
634 and 3) a slow non-linear fraction with $(\text{Si:Al}_{\text{aq}} / \text{Si:Al}_{\text{solid}}) = \pm 1$ indicates an initial
635 stoichiometric dissolution until edges are rounded (Table 3; Fig. 4). Re-analysis

636 with the NaOH method of isolated glass shards is consistent with a constant and
637 stoichiometric dissolution of shards with time (Fig 5b). Unfortunately, chemical
638 pre-treatment with HCl and H₂O₂ has affected the dissolution characteristics of
639 the shards creating an initial more rapid release of Si and Al.

640

641 We propose that acidic conditions during the cleaning procedure lead to partial
642 dissolution of the volcanic glass shards as shown by Wolff-Boenisch et al. (2004)
643 in acidic and far-from-equilibrium conditions for a range of shards (low and high
644 SiO₂ content). The process at acid conditions can be equally described as for
645 alkaline solutions through the two phase process of deprotonation of Al followed
646 by liberation of Si (Oelkers and Gislason, 2001). However, Al is preferentially
647 released due to the formation of a silica gel layer at pH < 9 with a thickness
648 depending on the exposure time to acids (Pollard et al., 2003). Of course,
649 addition to an alkaline environment led to a rapid dissolution of any enriched
650 silica gel coating. This provides an explanation for the high Si:Al_x ratios and rapid
651 Si release rates after pre-treatment (Table 4). We advise against chemical pre-
652 treatment when analyzing for BSi, because it causes the extraction of non-
653 biogenic fractions.

654

655 4.2.2 Discerning a shard signature from non-biogenic Si_{Alk}

656 In group 2 and 3 (Fig. 2), multiple non-linear fractions were observed when
657 modeling dissolution curves. We attribute the contribution of shards to the Si_{Alk}
658 fraction that evolves slowest to constant release (i.e. lowest k) while a low Si:Al_x
659 ratio suggests a non-biogenic source for the more rapid second Si_{Alk} fraction.

660

661 Group 2 and 3 are samples from lake, soil and peat records. Here, shards are
662 mixed with a variety of materials during deposition including organic carbon,
663 minerals and siliceous organisms. The tephra samples with the highest
664 contribution of the secondary Si_{Alk} fraction (e.g. Katla, Reykjanes, Saksunarvatn,
665 basaltic part of the Vedde Ash) have a lower stability according to Pollard's
666 theoretical stability modeling (2003). Likewise, the Parker index value for the
667 Tuhua tephra indicates a higher propensity for rapid weathering (Lowe, 1988).

Wim Clymans 8/5/2015 12:12

Deleted: modelling

669 We suggest that enhanced weathering in these environments leads to the
670 formation of secondary mineral and nanocrystalline fractions (Hodder et al.,
671 1990). This would create an additional non-biogenic, alkaline extractable source.
672 Such weathering products are typically enriched in Al with structural Si:Al_x
673 ratios between 1-3 for clay minerals (Dixon and Weed, 1989) and below 1 for
674 nanocrystalline structures (Levard et al., 2012). In fact, they dissolve or release
675 Si and Al more rapidly, and sometimes incongruently, at the beginning of a NaOH
676 extraction (Hashimoto and Jackson, 1958; Koning et al., 2002). This explains why
677 we observe a large range in Si:Al_x ratios (0.5-4) initially during the extraction.
678 We suggest it either represents the non-linear part of clay dissolution (Si:Al_x
679 ratio: 1-4) or complete dissolution of nanocrystalline minerals (Si:Al_x ratio: 0.5-
680 1).

681

682 Clay minerals will dissolve at a constant rate after an initial rapid release
683 (Koning et al., 2002) similar to primary glass shards. Consequently, the linear
684 part of the dissolution will reflect stoichiometric dissolution of glass shards
685 (Si:Al_{min} ratio: 3-5) and clay minerals (Si:Al_{min} ratio: 1-3). Samples with increased
686 abundance of clay contribution will have lowered Si:Al_{min} ratios compared to un-
687 weathered shards (Fig. 4.a).

688

689 **4.2.3 Discerning a shard signature from biogenic Si_{Alk}**

690 In group 3, higher Si:Al_x ratios > 5 for the slower fraction suggest the presence of
691 an additional biogenic Si_{Alk} fraction. Biogenic fractions including diatoms, sponge
692 spicules and phytoliths were identified in these samples microscopically. BSi
693 measurements of the separated biogenic fraction using the continuous NaOH
694 methodology had a single non-linear Si_{Alk} fraction, except Tuhua, with on average
695 72 wt% SiO₂. This fraction contains negligible amounts of Al and mineral
696 dissolution is absent confirming the biogenic nature of the separated material.
697 The combined presence of diatoms and sponge spicules in the Tuhua samples
698 explains the observation of two distinct BSi fractions (based on reactivity), as
699 alkaline dissolution rates are known to vary between different siliceous
700 organisms (Conley and Schelske, 2001).

701

702 Hence, it seems that the rounding of glass shards overlaps with the dissolution of
703 biogenic material, having similar reactivity but higher Si:Al_x ratios. The distinct
704 pattern of pure shards can be used to make a minimum estimate of its
705 contribution to the slower reacting fraction. Identification of glass shards'
706 dissolution behavior is essential to evaluate the methods ability to estimate the
707 biogenic Si_{Alk} content and evaluate the relative contribution of shard dissolution
708 to Si_{Alk}. The separation is based on the near to one ratio between Si:Al_x with the
709 Si:Al_{Solid} (Fig. 4).

710

711 **Figure 5**

712

713 Assumption 1: Si:Al corresponding to the slow fraction (Si_{Alk,1}) equals the Si:Al of
714 shards

715

$$\text{OR}$$
$$\left(\frac{\text{Si}}{\text{Al}}\right)_1 \approx \left(\frac{\text{Si}}{\text{Al}}\right)_{\text{Solid}}$$

716

717

718 Assumption 2: All Al originates from shards for the slow fraction i.e. no Al release
719 from the biogenic fraction. This leads to an overestimation of Al as small
720 amounts (< 0.05 wt%) of Al are found in phytoliths and diatoms (Kameník et al.,
721 2013; Van Cappellen et al., 2002).

722

$$Al_1 = Al_{Bsi} + Al_{Solid} \text{ with } Al_{Bsi} = 0$$

723 So,

$$Al_1 = Al_{Solid}$$

724

725 The Si coming from shards can then be calculated by substitution:

$$Si_{Solid} = \left(\frac{\text{Si}}{\text{Al}}\right)_{\text{Solid}} \cdot Al_1$$

726

727 We know that,

728

$$Si_1 = Si_{BSi} + Si_{Solid}$$

729 This delivers:

$$Si_{BSi} = Si_1 - Si_{Solid}$$

730

731 The results of this separation exercise combined with the observed difference in
732 other fractions are provided in Figure 5. Significant shards contribution to Si_{Alk} is
733 observed for all samples except Reclus R₁. Although we have no definitive
734 explanation why our Reclus R₁ sample did not contain observable amounts of
735 shards, our results support the physical observation of no retrievable shard
736 fraction by heavy liquid separation. If anything, it supports the appropriateness
737 of the chemical analysis to detect the occurrence of shards.

738

739 Initial dissolution of shard edges varies between 0.1 to 8 wt% SiO₂ with a median
740 contribution of 1.8 wt% SiO₂. The variation in contribution depends on how
741 fragmented and weathered (i.e. partially dissolved) the glass shards are. There
742 will be a decrease in its contribution if edges have been smoothed during natural
743 dissolution processes. It shows that dissolution of glass shards can contribute
744 substantially to the determination of BSi [when BSi concentrations are low](#).
745 Likewise, the non-biogenic Si sources (defined as “minerals” here) contribute
746 between 0.2 to 5 wt% SiO₂ with a median contribution equal to 0.89 wt% SiO₂.
747 The combined effect potentially exceeds the biogenic fraction (e.g. K1500), while
748 for others it contributes to less than 10% of the total extracted Si pool (e.g.
749 Armor1000 and Reclus R₁).

750

751 **4.3 The tephra factor in soil and paleoecological studies**

752 **4.3.1 Implications for soil scientists**

753 The global median Si_{Alk} in the top 1m of the soil column using alkaline extraction
754 techniques ranges between 0.79-1.12 wt% SiO₂ (e.g. Melzer et al., 2012; Saccone
755 et al., 2007; Sommer et al., 2013). The magnitude overlaps with Si_{Alk} content
756 attributed to tephra, to the initial rapid dissolution of clay minerals and/or
757 complete dissolution of nanocrystalline fractions in our experiments (Fig. 5). A

758 similar magnitude of Si release between soil samples and our untreated tephra
759 samples during alkaline extraction, implies that the combined dissolution of
760 glass shards, and their weathering products, if present, can disguise for a limited
761 amount of settings the environmental signal of the BSi proxy.

762
763 Glass shards are an important direct source of methodological bias in tephra-
764 based soils, that include Andosols (ISSS-ISRIC-FAO, 1998). Andosols have a
765 limited spatial extent covering about 1-2% of the land surface. Likewise, volcanic
766 bedrock formed at the surface covers 6.6% of the land surface (Hartmann and
767 Moosdorf, 2012) and is known to contain limited amounts of glass shards, which
768 are a potential source of Si_{Alk} in soils. Further, glass shards can be an important
769 component of soils developed in aeolian deposits in the Great Plains, USA
770 (Reyerson, 2012). The inheritance of glass shards in some types of aeolian
771 material might partly explain high Si_{Alk} in aeolian deposits measured by other
772 studies (e.g. 4 wt% SiO₂; Saccone et al., 2007).

773
774 Better knowledge of the mineralogical composition of our samples could
775 improve classification of the non-biogenic fractions. Weathering products of
776 glass shards are proposed to be the largest contributor to the Si_{Alk} fraction. A
777 Si:Al_x ratio between 0.39 and 1.02 (5 out of 8 samples) for this fraction suggest
778 its source to be nanocrystalline fractions. These fractions are typically described
779 as allophanes and imogolites with a Si:Al_x ratio between 0.5-1 (Levard et al.,
780 2012), and dissolve completely within the first 5 minutes of alkaline extraction
781 (Hashimoto and Jackson, 1958; Kamatani and Oku, 2000). Various studies have
782 shown that these nanocrystalline minerals also develop in soils without a
783 volcanic origin (Gustafsson et al., 1999; Parfitt, 2009). For example, in podzols
784 supersaturation of Al species at ambient dissolved Si concentration leads to the
785 formation of allophanes and imogolites. Nanocrystalline structures are stable at
786 ambient pH conditions above 5 (Parfitt, 2009). Extraction of Si_{Alk} will include
787 them in the biological pools (Clymans et al., 2014) and lead to an overestimation
788 of BSi in both volcanic and non-volcanic soils at ambient pH conditions.

789

Wim Clymans 4/5/2015 11:28

Deleted: Limited k

Wim Clymans 4/5/2015 11:37

Deleted: have aided our

Wim Clymans 4/5/2015 11:34

Deleted: W

793 We recommend caution when interpreting Si_{Alk} measurements from Andosols, or
794 soils developed on volcanic bedrock, at sites where inheritance of volcanic
795 material through aeolian or water deposition is likely. The NaOH method (after
796 Koning et al., 2002) proved its ability to pinpoint problematic samples, and to
797 separate the biogenic from non-biogenic fractions. The method delivers an
798 excellent opportunity to improve the determination of BSi pools in soil profiles.

799 4.3.2 Implications for paleoecological studies

800 Biogenic silica, estimated as Si_{Alk} , has proven to be a valuable tool in
801 paleoecological studies as an indicator of environmental changes (e.g. changes in
802 productivity, climate, precipitation and nutrient supply). In lacustrine sediment
803 cores, BSi content can range from the detection limit (0.01 wt%) to >70 wt%
804 SiO_2 (Frings et al., 2014a). The downcore variations in BSi through time vary
805 from as little as 2 wt% SiO_2 (Adams and Finkelstein, 2010; Ampel et al., 2008) to
806 a high of 10-40 wt% SiO_2 (Johnson et al., 2011; Prokopenko et al., 2006; Van der
807 Putten et al., 2015) and depends on several interacting factors such as mineral
808 matter or organic matter accumulation, diatom productivity and
809 preservation/dissolution processes. Hence, these processes control the relative
810 effect that tephra constituents (<3 wt% SiO_2 , Fig. 5) have on Si_{Alk} determination.
811 In paleorecords, where there is a potential contribution of tephra combined with
812 low Si_{Alk} concentrations or small downcore variations in Si_{Alk} , the use of Si_{Alk} as
813 an environmental proxy should be used with caution.

814

815 The accuracy of the alkaline extraction methods as a proxy for BSi
816 concentrations in sediment will depend on the origin of the mineral matter.
817 Koning et al. (2002) suggested that good results with the NaOH method can be
818 obtained for BSi/clay ratios of about 0.005, whereas for Na_2CO_3 good values can
819 be obtained from a 0.02 ratio. We show that for tephra samples it is a bit more
820 complicated as rounding of the glass shards edges and dissolution of its
821 weathering products (i.e. nanocrystalline minerals and secondary minerals) also
822 contribute to the apparent BSi fraction. Obviously, the spatial and therefore
823 temporal extent of potential contribution is restricted to core sections
824 representing episodes of 1) direct tephra deposition, and subsequent in-situ

Wim Clymans 8/5/2015 11:26

Deleted: 2

826 reworking; or 2) indirect contribution through mobilization of tephra and its
827 weathering products in a tephra covered landscape.

828

829 Our study highlights a direct effect of tephra on quantification of BSi.

830 Additionally, tephra deposition in lakes and peatlands can alter the diatom
831 community composition and diatom abundance (Harper et al., 1986; Hickman
832 and Reasoner, 1994; Lotter et al., 1995), though, not always (Telford et al., 2004).

833 Tephra input can induce a change in water chemistry, causing altered diatom
834 growth and/or preservation (for a review see Harper et al., 1986). In such case,

835 the increase in BSi accumulation can be indirectly attributed to tephra
836 deposition rather than to environmental changes. The methods used in our study

837 cannot distinguish between tephra induced diatom blooms and those resulting
838 from short- or long-term environmental change. Nevertheless, zones in a

839 sediment record potentially prone to a tephra-induced bloom can be highlighted
840 based on reconnaissance of glass shard contributions. This research topic

841 warrants further investigation, and requires detailed analysis of high resolution

842 records known to be prone to volcanic inputs.

843

844 **4.3.3 Implications for pre-treatment steps of EPMA during** 845 **tephrochronological studies**

846 Tephrochronology requires geochemical fingerprinting of tephra through
847 electron probe microanalysis (EPMA) (Lowe, 2011). EPMA on tephra requires
848 that they are unaltered by natural or laboratory processes. Unfortunately, tephra
849 shards are sensitive to dissolution at high and low pH, conditions that are both
850 naturally occurring and frequently applied during pre-treatment (e.g. Blockley et
851 al., 2005; Dugmore et al., 1992). Therefore, corrosive chemical pre-treatment is
852 increasingly avoided in tephrochronological studies and has been replaced by
853 heavy liquid floatation protocols (Blockley et al., 2005; Turney, 1998). The use of
854 NaOH (typical 0.3M in tephra preparation studies) for cleaning tephra samples of
855 biogenic Si (Davies et al., 2003; Rose et al., 1996; Wulf et al., 2013) should be
856 used with great caution. Our study demonstrates that alkaline treatments lead to
857 severe dissolution of shards, and can negatively affect the reconnaissance of
858 shards for EPMA analysis. Our data show that dissolution of the shards was

Wim Clymans 8/5/2015 12:38

Deleted: T

Wim Clymans 8/5/2015 13:01

Deleted: but

Wim Clymans 8/5/2015 12:52

Deleted: Reported timeframes wherein sustained effects of tephra on diatom productivity can be observed varies between 7 yrs and more than 100 yrs (cit. Barsdate and Dugdale, 1972 in Hickman and Reasoner, 1994). This temporal resolution can only be obtained in systems with a high accumulation rate and an excellent chronological constraint, e.g. in varved records (Lotter et al., 1995). On longer timescales, the effect of tephra deposition will be minimized and consequently BSi remains a stable and valid proxy (Hickman and Reasoner, 1994; Johnson et al., 2011). .

... [1]

Wim Clymans 8/5/2015 12:26

Deleted: The

878 equivalent to 4 wt% SiO₂ in the first 40 minutes (Fig. 2.a) and that a complete
879 dissolution is attained in less than a day. The severity of the dissolution effect
880 depends on the duration of extraction, the temperature at which extraction is
881 performed and the molarity of the solution used (Müller and Schneider, 1993).
882 Good criteria for NaOH cleaning are that extraction times should 1) allow
883 complete BSi dissolution, and 2) limit shard dissolution to a maximum of 10 wt%
884 SiO₂ so that a sufficient number of undamaged shards remain for EPMA analysis.
885 Finally, the Si and Al data suggest stoichiometric dissolution of shards implying
886 that their geochemical composition will remain unaltered. We cannot be
887 conclusive as modeled Si:Al are too imprecise and the release of other dominant
888 constituents (e.g. Na, K) were not monitored. EPMA on samples before and after
889 alkaline treatment (preferentially NaOH) could resolve this issue.

890 **5 Conclusion**

891 Various wet chemical alkaline extraction techniques commonly used to measure
892 Si_{Aik} content have been criticized for their usefulness outside marine sciences.
893 Problems are attributed to dissolution of non-biogenic fractions and incomplete
894 dissolution of the biogenic fraction. We evaluated two alkaline extraction
895 techniques using 0.1 M Na₂CO₃ and 0.5 M NaOH solutions for measuring Si_{Aik} as a
896 proxy for environmental change in soil, peat and lake records with volcanic
897 inputs.

898

899 Alkaline extraction techniques should be used with caution in tephra-based soil
900 profiles, soils developed on volcanic bedrock or soils with aeolian input
901 containing volcanic material. The influence of the dissolution of glass shards on
902 BSi measurements in paleoecological records can be significant in oligotrophic
903 environments with a low BSi sediment content. Here, concomitant accumulation
904 of volcanic material will lead to significant contribution of a non-biogenic
905 fraction during the determination of Si_{Aik}. Otherwise, Si_{Aik} determined with
906 traditional alkaline methods can be freely used as a proxy to evaluate
907 environmental changes, especially when part of multi-proxy studies.

908

Wim Clymans 8/5/2015 13:08

Deleted: a

910 Determination of the time course of dissolution during the first 5 hours of
911 extraction using 0.1 M Na₂CO₃ has proven to be a sensitive indicator of other
912 forms of Si_{Alk}. In addition, the sequential Na₂CO₃ extraction is a rather simple
913 method and the results show a high recovery of the biogenic Si fraction (Meunier
914 et al., 2014; Saccone et al., 2007). The main advantage of the method is that a
915 relatively large number of samples can be measured in a relatively short time
916 span. In environments with a high BSi content, the 0.1 M Na₂CO₃ method is the
917 preferred one.

918

919 We also show that the continuous monitoring of Si and Al extraction in NaOH
920 addresses the main disadvantages of the sequential Na₂CO₃ method. Our analysis
921 of pure tephra (i.e. mainly containing glass shards) samples provided important
922 information about the dissolution characteristics of volcanic glass shards. Our
923 study confirms that the dissolution of tephra contributes to Si_{Alk} determination,
924 but the distinct signature of glass shard dissolution can help to isolate its
925 contribution to the biogenic fraction. Continuous monitoring of Si and Al is
926 promoted to analyze complex samples from any environmental record to reduce
927 uncertainty on biological reactive fractions. Future studies should address the
928 reliability and precision of the separation of different fractions through **modeling**
929 of dissolution parameters.

930

931 **Acknowledgments:**

932 The following people are thanked for their invaluable assistance: S.R. Gíslason
933 for providing fresh tephra (Eyjafjallajökull). A. Cools, D.U. Delmonte for
934 assistance during the continuous extractions. A. Gosh helping with microscopic
935 analysis. G. Fontorbe, P. Abbott, S. Davies for advice on sample preparation.
936 Comments by P. Frings, G. Fontorbe, H. Alfredsson, B. Alvarez de Glasby, and J.
937 Stadmark improved the manuscript. **Likewise, the editor, anonymous reviewers**
938 **and D.J. Lowe are thanked for their constructive comments and suggestions.** This
939 research was funded by the Knut & Alice Wallenberg Foundation, FWO en Belspo
940 (SOGLO). LB thanks Special Research Funding from the University of Antwerp
941 (BOF-UA and NOI) for the PhD fellowship funding.

942

Wim Clymans 8/5/2015 13:09

Deleted: modelling

Wim Clymans 8/5/2015 14:45

Formatted: No widow/orphan control,
Don't adjust space between Latin and
Asian text, Don't adjust space between
Asian text and numbers

Wim Clymans 4/5/2015 09:45

Deleted:

945 **Author contributions:**

946 WC, NVdP, DJC were responsible for the concept and design of this study. SW, SB,
947 NVdP, BM and GG advised on, and helped with sample collection. WC, LB and
948 NVdP prepared and analyzed samples. WC was responsible for data analysis and
949 interpretation with inputs on methodology of LB, ES and DJC, and interpretation
950 of paleoecological data by all other authors. WC provided a first draft. All authors
951 contributed to the writing of the paper.

952

953

954

955 **References:**

956 Adams, J. K., and Finkelstein, S. A.: Watershed-scale reconstruction of middle and
957 late Holocene paleoenvironmental changes on Melville Peninsula, Nunavut,
958 Canada, *Quaternary Sci Rev*, 29, 2302-2314, 10.1016/j.quascirev.2010.05.033,
959 2010.

960 Ampel, L., Wohlfarth, B., Risberg, J., and Veres, D.: Paleolimnological response to
961 millennial and centennial scale climate variability during MIS 3 and 2 as
962 suggested by the diatom record in Les Echets, France, *Quaternary Sci Rev*, 27,
963 1493-1504, 10.1016/j.quascirev.2008.04.014, 2008.

964 Andresen, C. S., Björck, S., Bennike, O., and Bond, G.: Holocene climate changes in
965 southern Greenland: evidence from lake sediments, *J Quaternary Sci*, 19, 783-
966 795, 10.1002/jqs.886, 2004.

967 Barão, L., Clymans, W., Vandevenne, F., Meire, P., Conley, D., and Struyf, E.:
968 Pedogenic and biogenic alkaline - extracted silicon distributions along a
969 temperate land - use gradient, *Eur J Soil Sci*, 65, 693-705, 2014.

970 Barão, A., Vandevenne, F., Clymans, W., Frings, P., Ragueneau, O., Meire, P.,
971 Conley, D. J., and Struyf, E.: Alkaline-extractable silicon from land to ocean: a
972 challenge for biogenic Silicon determination, *Limnology and Oceanography:*
973 *Methods*, In press, 2015.

974 Björck, S., Rittenour, T., Rosén, P., França, Z., Möller, P., Snowball, I., Wastegård, S.,
975 Bennike, O., and Kromer, B.: A Holocene lacustrine record in the central North
976 Atlantic: proxies for volcanic activity, short-term NAO mode variability, and long-
977 term precipitation changes, *Quaternary Sci Rev*, 25, 9-32,
978 <http://dx.doi.org/10.1016/j.quascirev.2005.08.008>, 2006.

979 Blockley, S. P. E., Pyne-O'Donnell, S. D. F., Lowe, J. J., Matthews, I. P., Stone, A.,
980 Pollard, A. M., Turney, C. S. M., and Molyneux, E. G.: A new and less destructive
981 laboratory procedure for the physical separation of distal glass tephra shards
982 from sediments, *Quaternary Sci Rev*, 24, 1952-1960,
983 10.1016/j.quascirev.2004.12.008, 2005.

984 Churchman, J., and Lowe, D. J.: Alteration, formation, and occurrence of minerals
985 in soils, 2nd ed., *Handbook of Soil Sciences. Vol. 1: Properties and Processes*,
986 edited by: Huang, P., and Li, Y., CRC Press, 2012.

Wim Clymans 8/5/2015 13:29

Deleted: .

- 988 Clymans, W., Govers, G., Van Wesemael, B., Meire, P., and Struyf, E.: Amorphous
989 silica analysis in terrestrial runoff samples, *Geoderma*, 2011a.
- 990 Clymans, W., Struyf, E., Govers, G., Vandevenne, F., and Conley, D. J.:
991 Anthropogenic impact on amorphous silica pools in temperate soils,
992 *Biogeosciences*, 8, 2281-2293, 10.5194/bg-8-2281-2011, 2011b.
- 993 Clymans, W., Lehtinen, T., Gísladóttir, G., Lair, G., Barão, L., Ragnarsdóttir, K.,
994 Struyf, E., and Conley, D.: Si Precipitation During Weathering in Different
995 Icelandic Andosols, *Procedia Earth Planet Sci*, 10, 260-265, 2014.
- 996 Conley, D., Schelske, C., and Stoermer, E.: Modification of the biogeochemical
997 cycle of silica with eutrophication, *Mar Ecol Prog Ser*, 101, 179-192, 1993.
- 998 Conley, D., and Schelske, C.: Biogenic silica, in: *Tracking Environmental Change*
999 *Using Lake Sediments: Biological Methods and Indicators*, edited by: Smol, J.,
1000 Birks, H., and Last, W., Kluwer Academic Press, 281-293, 2001.
- 1001 Cornelis, J.-T., Titeux, H., Ranger, J., and Delvaux, B.: Identification and
1002 distribution of the readily soluble silicon pool in a temperate forest soil below
1003 three distinct tree species, *Plant Soil*, 342, 369-378, 10.1007/s11104-010-0702-
1004 x, 2011a.
- 1005 Cornelis, J. T., Ranger, J., Iserentant, A., and Delvaux, B.: Tree species impact the
1006 terrestrial cycle of silicon through various uptakes, *Biogeochemistry*, 97, 231-
1007 245, 10.1007/s10533-009-9369-x, 2010.
- 1008 Cornelis, J. T., Delvaux, B., Georg, R. B., Lucas, Y., Ranger, J., and Opfergelt, S.:
1009 Tracing the origin of dissolved silicon transferred from various soil-plant
1010 systems towards rivers: a review, *Biogeosciences*, 8, 89-112, 2011b.
- 1011 Davies, S. M., Wastegård, S., and Wohlfarth, B.: Extending the limits of the
1012 Borrobol Tephra to Scandinavia and detection of new early Holocene tephra,
1013 *Quaternary Res*, 59, 345-352, 2003.
- 1014 DeMaster, D.: The supply and accumulation of silica in the marine-environment,
1015 *Geochim Cosmochim Acta*, 45, 1715-1732, 1981.
- 1016 Dixon, J. B., and Weed, S. B.: *Minerals in soil environments*, 2nd ed., *Minerals in*
1017 *soil environments*, Soil Sci Soc Am J, Madison, Wisconsin, USA, 1989.
- 1018 Dugmore, A. J., Newton, A. J., Sugden, D. E., and Larsen, G.: Geochemical stability
1019 of fine-grained silicic Holocene tephra in Iceland and Scotland, *J Quaternary Sci*,
1020 7, 173-183, 10.1002/jqs.3390070208, 1992.
- 1021 Fernández, M., Björck, S., Wohlfarth, B., Maidana, N. I., Unkel, I., and Van der
1022 Putten, N.: Diatom assemblage changes in lacustrine sediments from Isla de los
1023 Estados, southernmost South America, in response to shifts in the southwesterly
1024 wind belt during the last deglaciation, *J Paleolimnol*, 50, 433-446,
1025 10.1007/s10933-013-9736-4, 2013.
- 1026 Frings, P., Clymans, W., Jeppesen, E., Lauridsen, T., Struyf, E., and Conley, D.: Lack
1027 of steady-state in the global biogeochemical Si cycle: emerging evidence from
1028 lake Si sequestration, *Biogeochemistry*, 117, 255-277, 10.1007/s10533-013-
1029 9944-z, 2014a.

- 1030 Frings, P. J., Clymans, W., and Conley, D. J.: Amorphous Silica Transport in the
 1031 Ganges Basin: Implications for Si Delivery to the Oceans, *Procedia Earth Planet*
 1032 *Sci*, 10, 271-274, 2014b.
- 1033 Gehlen, M., and van Raaphorst, W.: Early diagenesis of silica in sandy North sea
 1034 sediments: quantification of the solid phase, *Mar Chem*, 42, 71-83,
 1035 [http://dx.doi.org/10.1016/0304-4203\(93\)90238-J](http://dx.doi.org/10.1016/0304-4203(93)90238-J), 1993.
- 1036 Gísladóttir, G., Erlendsson, E., Lal, R., and Bigham, J.: Erosional effects on
 1037 terrestrial resources over the last millennium in Reykjanes, southwest Iceland,
 1038 *Quaternary Res*, 73, 20-32, <http://dx.doi.org/10.1016/j.yqres.2009.09.007>,
 1039 2010.
- 1040 Gislason, S. R., Alfredsson, H. A., Eiriksdóttir, E. S., Hassenkam, T., and Stipp, S. L.
 1041 S.: Volcanic ash from the 2010 Eyjafjallajökull eruption, *Appl Geochem*, 26, S188-
 1042 S190, [10.1016/j.apgeochem.2011.03.100](http://dx.doi.org/10.1016/j.apgeochem.2011.03.100), 2011a.
- 1043 Gislason, S. R., Hassenkam, T., Nedel, S., Bovet, N., Eiriksdóttir, E. S., Alfredsson, H.
 1044 A., Hem, C. P., Balogh, Z. I., Dideriksen, K., Oskarsson, N., Sigfusson, B., Larsen, G.,
 1045 and Stipp, S. L.: Characterization of Eyjafjallajökull volcanic ash particles and a
 1046 protocol for rapid risk assessment, *P Natl Acad Sci USA*, 108, 7307-7312,
 1047 [10.1073/pnas.1015053108](http://dx.doi.org/10.1073/pnas.1015053108), 2011b.
- 1048 Grasshoff, K., Ehrhardt, M., and Kremling, K.: *Methods of Sea Water Analysis*, 314,
 1049 1983.
- 1050 Gudmundsson, A., Oskarsson, N., Grönvold, K., Saemundsson, K., Sigurdsson, O.,
 1051 Stefansson, R., Gislason, S., Einarsson, P., Brandsdóttir, B., Larsen, G.,
 1052 Johannesson, H., and Thordarson, T.: The 1991 eruption of Hekla, Iceland, *B*
 1053 *Volcanology*, 54, 238-246, [10.1007/BF00278391](http://dx.doi.org/10.1007/BF00278391), 1992.
- 1054 Guntzer, F., Keller, C., and Meunier, J.-D.: Benefits of plant silicon for crops: a
 1055 review, *Agron Sustain Dev*, 32, 201-213, 2012.
- 1056 Gustafsson, J. P., Bhattacharya, P., and Karlton, E.: Mineralogy of poorly
 1057 crystalline aluminium phases in the B horizon of Podzols in southern Sweden,
 1058 *Appl Geochem*, 14, 707-718, [http://dx.doi.org/10.1016/S0883-2927\(99\)00002-](http://dx.doi.org/10.1016/S0883-2927(99)00002-5)
 1059 [5](http://dx.doi.org/10.1016/S0883-2927(99)00002-5), 1999.
- 1060 Hafliðason, H., Larsen, G., and Ólafsson, G.: The Recent Sedimentation History of
 1061 Thingvallavatn, Iceland, *Oikos*, 64, 80-95, [10.2307/3545044](http://dx.doi.org/10.2307/3545044), 1992.
- 1062 Harper, M. A., Howorth, R., and McLeod, M.: Late Holocene diatoms in Lake
 1063 Poukawa: Effects of airfall tephra and changes in depth, *New Zeal J Mar Fresh*,
 1064 20, 107-118, [10.1080/00288330.1986.9516135](http://dx.doi.org/10.1080/00288330.1986.9516135), 1986.
- 1065 Hartmann, J., and Moosdorf, N.: The new global lithological map database GLiM:
 1066 A representation of rock properties at the Earth surface, *Geochem Geophys Geosy*,
 1067 13, 2012.
- 1068 Hashimoto, I., and Jackson, M.: Rapid dissolution of allophane and kaolinite-
 1069 halloysite after dehydration, *Natl. Conf. on Clays and Clay Minerals*, 7th,
 1070 Washington, 1958, 102-113,
- 1071 Heathcote, A., Ramstack Hobbs, J., Anderson, N. J., Frings, P., Engstrom, D., and
 1072 Downing, J.: Diatom floristic change and lake paleoproduction as evidence of

Stefan 19/5/2015 17:29

Deleted: o

Stefan 19/5/2015 17:29

Deleted: o

- 1075 recent eutrophication in shallow lakes of the midwestern USA, *J Paleolimnol*, 1-
1076 18, 10.1007/s10933-014-9804-4, 2014.
- 1077 Heyng, A. M., Mayr, C., Lücke, A., Striewski, B., Wastegård, S., and Wissel, H.:
1078 Environmental changes in northern New Zealand since the Middle Holocene
1079 inferred from stable isotope records ($\delta^{15}\text{N}$, $\delta^{13}\text{C}$) of Lake Pupuke, *J Paleolimnol*,
1080 48, 351-366, 10.1007/s10933-012-9606-5, 2012.
- 1081 Hickman, M., and Reasoner, M. A.: Diatom responses to late Quaternary
1082 vegetation and climate change, and to deposition of two tephras in an alpine and
1083 a sub-alpine lake in Yoho National Park, British Columbia, *J Paleolimnol*, 11, 173-
1084 188, 1994.
- 1085 Hodder, A., Green, B., and Lowe, D.: A two-stage model for the formation of clay
1086 minerals from tephra-derived volcanic glass, *Clay Miner*, 25, 313-327, 1990.
- 1087 Hydes, D., and Liss, P.: Fluorimetric method for the determination of low
1088 concentrations of dissolved aluminium in natural waters, *Analyst*, 101, 922-931,
1089 1976.
- 1090 ISSS-ISRIC-FAO: World Reference Base for Soil Resources, World Soil Resources
1091 Reports, edited by: FAO, Rome, 1998.
- 1092 | Johansson, H., [Lind, E.M.](#) and Wastegård, S.: Proximal tephra glass geochemistry
1093 from eruptions in the Azores archipelago and possible links with sites in Ireland,
1094 [The Holocene](#), submitted.
- 1095 Johnson, T. C., Brown, E. T., and Shi, J.: Biogenic silica deposition in Lake Malawi,
1096 East Africa over the past 150,000years, *Palaeogeogr Palaeocl*, 303, 103-109,
1097 10.1016/j.palaeo.2010.01.024, 2011.
- 1098 Kamatani, A., and Oku, O.: Measuring biogenic silica in marine sediments, *Mar*
1099 *Chem*, 68, 219-229, 2000.
- 1100 Kameník, J., Mizera, J., and Řanda, Z.: Chemical composition of plant silica
1101 phytoliths, *Environ Chem Lett*, 11, 189-195, 10.1007/s10311-012-0396-9, 2013.
- 1102 Koning, E., Epping, E., and Van Raaphorst, W.: Determining biogenic silica in
1103 marine samples by tracking silicate and aluminium concentrations in alkaline
1104 leaching solutions, *Aquat Geochem*, 8, 37-67, 2002.
- 1105 Le Bas, M., Le Maitre, R., Streckeisen, A., and Zanettin, B.: A chemical classification
1106 of volcanic rocks based on the total alkali-silica diagram, *J Petrol*, 27, 745-750,
1107 1986.
- 1108 [Leinen, M.: Normative calculation technique for determining opal in deep-sea](#)
1109 [sediments, *Geochim Cosmochim Acta*, 41, 671-676, 1977.](#)
- 1110 Levard, C., Doelsch, E., Basile-Doelsch, I., Abidin, Z., Miche, H., Masion, A., Rose, J.,
1111 Borschneck, D., and Bottero, J. Y.: Structure and distribution of allophanes,
1112 imogolite and proto-imogolite in volcanic soils, *Geoderma*, 183-184, 100-108,
1113 10.1016/j.geoderma.2012.03.015, 2012.
- 1114 Lind, E. M., and Wastegård, S.: Tephra horizons contemporary with short early
1115 Holocene climate fluctuations: new results from the Faroe Islands, *Quatern Int*,
1116 246, 157-167, 2011.

Wim Clymans 21/5/2015 11:46

Deleted: .

- 1118 Lotter, A., Birks, H., and Zolitschka, B.: Late-glacial pollen and diatom changes in
1119 response to two different environmental perturbations: volcanic eruption and
1120 Younger Dryas cooling, *J Paleolimnol*, 14, 23-47, 1995.
- 1121 Lowe, D. J.: Stratigraphy, age, composition, and correlation of late Quaternary
1122 tephra interbedded with organic sediments in Waikato lakes, North Island, New
1123 Zealand, *New Zealand journal of geology and geophysics*, 31, 125-165, 1988.
- 1124 Lowe, D. J.: Tephrochronology and its application: A review, *Quat Geochronol*, 6,
1125 107-153, 10.1016/j.quageo.2010.08.003, 2011.
- 1126 Lyle, A. O., and Lyle, M.: Determination of biogenic opal in pelagic marine
1127 sediments: a simple method revisited, *Proceedings of the Ocean Drilling
1128 Program, Initial Reports*, 2002, 1-21,
- 1129 Mackie, E. A., Davies, S. M., Turney, C. S., Dobbyn, K., Lowe, J. J., and Hill, P. G.: The
1130 use of magnetic separation techniques to detect basaltic microtephra in last
1131 glacial-interglacial transition (LGIT; 15–10 ka cal. bp) sediment sequences in
1132 Scotland, *Scot J Geol*, 38, 21-30, 2002.
- 1133 Melzer, S. E., Chadwick, O. A., Hartshorn, A. S., Khomo, L. M., Knapp, A. K., and
1134 Kelly, E. F.: Lithologic controls on biogenic silica cycling in South African savanna
1135 ecosystems, *Biogeochemistry*, 108, 317-334, 2012.
- 1136 Meunier, J. D., Keller, C., Guntzer, F., Riotte, J., Braun, J. J., and Anupama, K.:
1137 Assessment of the 1% Na₂CO₃ technique to quantify the phytolith pool,
1138 *Geoderma*, 216, 30-35, 10.1016/j.geoderma.2013.10.014, 2014.
- 1139 [Meyer-Jacob, C., Vogel, H., Boxberg, F., Rosén, P., Weber, M. E., and Bindler, R.:
1140 Independent measurement of biogenic silica in sediments by FTIR spectroscopy
1141 and PLS regression, *Journal of Paleolimnology*, 52, 245-255, 2014.](#)
- 1142 Morley, D. W., Leng, M. J., Mackay, A. W., Sloane, H. J., Rioual, P., and Battarbee, R.
1143 W.: Cleaning of lake sediment samples for diatom oxygen isotope analysis, *J
1144 Paleolimnol*, 31, 391-401, 2004.
- 1145 Müller, P., and Schneider, R.: An automated leaching method for the
1146 determination of opal in sediments and particulate matter, *Deep-Sea Res PT I*,
1147 40, 425-444, 1993.
- 1148 Norddahl, H., and Hafliðason, H.: The Skogar tephra, a Younger Dryas marker in
1149 north Iceland, *Boreas*, 21, 23-41, 1992.
- 1150 Oelkers, E. H., and Gislason, S. R.: The mechanism, rates and consequences of
1151 basaltic glass dissolution: I. An experimental study of the dissolution rates of
1152 basaltic glass as a function of aqueous Al, Si and oxalic acid concentration at 25 C
1153 and pH= 3 and 11, *Geochim Cosmochim Ac*, 65, 3671-3681, 2001.
- 1154 [Ohlendorf, C., and Sturm, M.: A modified method for biogenic silica
1155 determination, *Journal of Paleolimnology*, 39, 137-142, 2008.](#)
- 1156 Parfitt, R.: Allophane and imogolite: role in soil biogeochemical processes, *Clay
1157 Miner*, 44, 135-155, 2009.
- 1158 Pollard, A., Blockley, S., and Ward, K.: Chemical alteration of tephra in the
1159 depositional environment: theoretical stability modelling, *J Quaternary Sci*, 18,
1160 385-394, 2003.

- 1161 Prokopenko, A. A., Hinnov, L. A., Williams, D. F., and Kuzmin, M. I.: Orbital forcing
1162 of continental climate during the Pleistocene: a complete astronomically tuned
1163 climatic record from Lake Baikal, SE Siberia, *Quaternary Sci Rev*, 25, 3431-3457,
1164 2006.
- 1165 Reyerson, P.: Reactive Silica in Loess-Derived Soils of Central North America,
1166 Doctor of Philosophy, Geography, University of Wisconsin-Madison, 187 pp.,
1167 2012.
- 1168 Rose, N., Golding, P., and Battarbee, R.: Selective concentration and enumeration
1169 of tephra shards from lake sediment cores, *The Holocene*, 6, 243-246, 1996.
- 1170 Saccone, L., Conley, D., Koning, E., Sauer, D., Sommer, M., Kaczorek, D., Blecker, S.,
1171 and Kelly, E.: Assessing the extraction and quantification of amorphous silica in
1172 soils of forest and grassland ecosystems, *Eur J Soil Sci*, 58, 1446-1459, 2007.
- 1173 Sauer, D., Saccone, L., Conley, D., Herrmann, L., and Sommer, M.: Review of
1174 methodologies for extracting plant-available and amorphous Si from soils and
1175 aquatic sediments, *Biogeochemistry*, 80, 89-108, 2006.
- 1176 Sommer, M., Jochheim, H., Höhn, A., Breuer, J., Zagorski, Z., Busse, J., Barkusky, D.,
1177 Meier, K., Puppe, D., and Wanner, M.: Si cycling in a forest biogeosystem—the
1178 importance of transient state biogenic Si pools, *Biogeosciences*, 10, 4991-5007,
1179 2013.
- 1180 Stephens, J. C., and Hering, J. G.: Factors affecting the dissolution kinetics of
1181 volcanic ash soils: dependencies on pH, CO₂, and oxalate, *Appl Geochem*, 19,
1182 1217-1232, 2004.
- 1183 Struyf, E., and Conley, D.: Emerging understanding of the ecosystem silica filter,
1184 *Biogeochemistry*, 107, 9-18, 2012.
- 1185 Telford, R. J., Barker, P., Metcalfe, S., and Newton, A.: Lacustrine responses to
1186 tephra deposition: examples from Mexico, *Quaternary Sci Rev*, 23, 2337-2353,
1187 2004.
- 1188 Turney, C. S.: Extraction of rhyolitic component of Vedde microtephra from
1189 minerogenic lake sediments, *J Paleolimnol*, 19, 199-206, 1998.
- 1190 Unkel, I., Björck, S., and Wohlfarth, B.: Deglacial environmental changes on Isla de
1191 los Estados (54.4 S), southeastern Tierra del Fuego, *Quaternary Sci Rev*, 27,
1192 1541-1554, 2008.
- 1193 Van Cappellen, P., Dixit, S., and van Beusekom, J.: Biogenic silica dissolution in the
1194 oceans: Reconciling experimental and field - based dissolution rates, *Global
1195 Biogeochem Cy*, 16, 23-21-23-10, 2002.
- 1196 [Van der Putten, N., Verbruggen, C., Björck, S., Michel, E., Disnar, J.-R., Chapron, E.,
1197 Moine, B. N. and de Beaulieu, J.-L.: The Last Termination in the South Indian
1198 Ocean: a unique terrestrial record from Kerguelen Islands \(49°S\) situated within
1199 the Southern Hemisphere westerly belt, *Quaternary Science Reviews*,
1200 \[10.1016/j.quascirev.2015.05.010\]\(#\), in press.](#)
- 1201 Verschuren, D., Johnson, T., Kling, H., Edgington, D., Leavitt, P., Brown, E., Talbot,
1202 M., and Hecky, R.: History and timing of human impact on Lake Victoria, East
1203 Africa, *Proc R Soc Lond B*, 269, 289-294, 2002.

Stefan 19/5/2015 16:09
Formatted: English (UK)

- 1204 Wastegård, S., Björck, S., Possnert, G., and Wohlfarth, B.: Evidence for the
1205 occurrence of Vedde Ash in Sweden: radiocarbon and calendar age estimates, *J*
1206 *Quaternary Sci*, 13, 271-274, 1998.
- 1207 Wolff-Boenisch, D., Gislason, S. R., Oelkers, E. H., and Putnis, C. V.: The dissolution
1208 rates of natural glasses as a function of their composition at pH 4 and 10.6, and
1209 temperatures from 25 to 74 C, *Geochim Cosmochim Ac*, 68, 4843-4858, 2004.
- 1210 Wulf, S., Ott, F., Słowiński, M., Noryskiewicz, A. M., Dräger, N., Martin-Puertas, C.,
1211 Czymzik, M., Neugebauer, I., Dulski, P., and Bourne, A. J.: Tracing the Laacher See
1212 Tephra in the varved sediment record of the Trzechowskie palaeolake in central
1213 Northern Poland, *Quaternary Sci Rev*, 76, 129-139, 2013.

Table 1 The provenance, origin of the sample, eruption date and composition of the specific tephra deposits analyzed.

Tephra	Origin	Profile	Age [#]	Composition	Reference
Hekla1991	Iceland	Fresh deposit	1991 AD	Basaltic-Andesite	Gudmundsson et al. 1992
EFJ2010_SJV	Iceland	Fresh deposit	2010 AD	Trachy-andesite	Unpublished data ^a
EFJ2010_1504	Iceland	Fresh deposit	2010 AD	Trachy-andesite	Gislason et al 2011a&b.
Fogo A	Azores, Portugal	Buried Soil	c. 5000 cal BP	Trachyte	Johansson et al, subm. ^b
PAS-2T39	Argentina	Lake	48742 cal BP	Rhyolite	Wastegård et al. 2013
TC09_48a	Kerguelen Island	Buried Soil	c. 1000 cal BP	Trachyte	Unpublished data ^c
Pompeii	Italy	Buried Soil	79 AD	Tephri-phonolite	Unpublished data ^d
Vedde Ash	Iceland	Fresh deposit	12100 cal BP	Mixed Basalt and Rhyolite	Norddahl & Hafliðason 1992 ^e
Reykjanes1226	Iceland	Soil	1226 AD	Basalt	Gísladóttir G. et al, 2010.
Cav-A	Azores, Portugal	Peat bog	1000 cal BP	Tephrite	Björck et al., 2006
Saksunarvatn	Faroe Island	Lake	10300 cal BP	Basalt	Lind & Wastegård, 2011 + Tephabase
Tuhua	New Zealand	Lake	7165 cal BP	Peralkaline Rhyolite	Heyng et al., 2012
Armor1000	Kerguelen Island	Peat bog	c. 1000 cal BP	Trachyte	Unpublished data ^e
Katla1500	Iceland	Soil	1500 AD	Basalt	Hafliðason et al., 1992
Reclus R ₁	Argentina	Lake	15000 cal BP	Rhyolite	Unkel et al. 2008

[#]Reported ages expressed as calendar years (AD), calibrated ¹⁴C ages (cal BP; BP being 1950 AD by convention) and approximations based on unpublished radiocarbon dates; [§] Referred to as the Skógar Tephra

^a Surface grab sample collected shortly after 2010 eruption at the south side in Seljavellir (N63°34'; W19°37'), and stored dried, used data Gislason et al. 2011b for typical ash; ^b Surface grab sample collected from the airfall deposit (N37°43'10.6; W25°30'0.96), stored dried. ^cSampled along a natural cut through the fluvial, volcano-sedimentary and peat deposits, at southeast of the Rallier du Baty Peninsula (S49°41'42"; E68°57'55"), dry pumices were extracted from the ignimbrite deposit and stored dried. ^dSample taken during archaeological investigation of Pompeii, quarter VI.30, room 2 (N40° 45'; E14° 29'), stored dried. ^eThe Armor peat sequence (S49°27.872; E69°43.484) was sampled by drilling in CALYPSO PVC tubes (φ = 11.5 cm), and stored cold (4°C) before freeze dried.

Deleted: (cal BP)

Wim Clymans 21/5/2015 11:46
Formatted ... [4]

Wim Clymans 21/5/2015 11:47
Formatted ... [3]

Wim Clymans 19/5/2015 12:11
Formatted Table ... [2]

Wim Clymans 19/5/2015 12:09
Deleted: 23*

Wim Clymans 19/5/2015 12:09
Deleted: 4*

Wim Clymans 19/5/2015 12:09
Deleted: 4*

Stefan 19/5/2015 17:31
Formatted ... [6]

Stefan 19/5/2015 17:31
Deleted: & Wastegård,...et al, in pre ... [7]

Stefan 19/5/2015 17:31
Formatted ... [8]

Wim Clymans 19/5/2015 12:09
Formatted ... [5]

Wim Clymans 8/5/2015 10:44
Deleted: Dacite

Wim Clymans 19/5/2015 12:10
Deleted: 48750

Wim Clymans 8/5/2015 10:48
Deleted: ^b

Wim Clymans 19/5/2015 12:10
Formatted ... [9]

Wim Clymans 8/5/2015 10:49
Formatted ... [10]

Wim Clymans 19/5/2015 12:10
Deleted: 1871

Wim Clymans 19/5/2015 12:11
Deleted: .

Wim Clymans 19/5/2015 12:10
Deleted: 722

Wim Clymans 19/5/2015 12:10
Deleted: 2

Wim Clymans 19/5/2015 12:11
Deleted: .

Wim Clymans 19/5/2015 12:11
Deleted: 7000

Wim Clymans 4/5/2015 11:30

Wim Clymans 19/5/2015 12:11
Formatted ... [11]

Wim Clymans 19/5/2015 12:11

Wim Clymans 5/5/2015 11:04

Table 2 Comparison of Si_{Alk} (wt%SiO₂ ± stdev; n=5) of 14 selected tephra deposits for two commonly applied methods: 0.1M Na₂CO₃ based on mineral dissolution slope 3-5hrs and 20-24hrs and 0.5M NaOH. Note: Sample EFJ2010_1504 is not included.

Name Tephra	3-5h Na ₂ CO ₃	20-24h Na ₂ CO ₃	NaOH	Si _{Alk,20-24h} / Si _{Alk,3-5h}
Hekla1991	0.49±0.27	2.75	0.27	5.61
EFJ2010_SJV	0.30±0.15	2.14±0.25	0.30	7.13
Fogo A	0.91±0.29	2.66±0.23	1.68	2.92
PAS-2T39	1.35±0.31	4.82	2.32	3.57
TC09_48a	1.13±0.27	6.00	4.34	5.31
Pompeii	1.08±0.05	2.73±0.46	0.90	2.53
Reykjanes1226	1.31±0.40	0.87	2.30	0.66
Vedde Ash	1.54±0.41	3.86	1.86	2.51
Saksunarvatn	5.82±1.13	8.23	5.57	1.41
Cav-A	1.13±0.19	1.91	1.60	1.69
Tuhua	7.73±0.59	14.00	10.53	1.81
Armor1000	4.09±0.37	4.96±1.09	3.51	1.21
Katla1500	2.18±0.48	3.39±1.04	4.89	1.56
Reclus R ₁	16.68±1.32	18.10	23.47	1.09

Table 3 Modeled dissolution parameters after alkaline (NaOH) extraction of untreated samples. For each fraction ($Si_{Alk,x}$; wt% SiO_2) the $Si:Al_x$ ratios, rate of non-linear dissolution/release k_x (min^{-1}) for fraction x and b (wt% SiO_2 min^{-1}) the slope of the mineral dissolution with a $Si:Al_{min}$ ratio are given for all samples. Additional column representing the Si and Al ratio of unweathered shards based on available EMPA data ($Si:Al_{solid}$).

Sample	Fraction 1			Fraction 2			Fraction 3			Mineral		Total	EMPA*
	$Si_{Alk,1}$	k_1	$Si:Al_1$	$Si_{Alk,2}$	k_2	$Si:Al_2$	$Si_{Alk,3}$	k_3	$Si:Al_3$	b	$Si:Al_{min}$	$Si_{Alk,tot}$	$Si:Al_{solid}$
Hekla1991	0.27	0.45	4.03	0.032	3.25	0.27	3.35
EFJ2010_SJV	0.30	0.15	3.41	0.027	4.08	0.30	3.41
EFJ2010_1504	1.24	0.16	3.53	0.116	3.59	1.24	3.44
Fogo A	1.68	0.11	3.98	0.108	3.12	1.68	3.44
PAS 2T39	2.32	0.11	4.92	0.130	4.17	2.32	4.89
TC09_48a	3.58	0.05	3.59	0.76	1.01	0.95	.	.	.	0.188	3.57	4.34	3.86
Pompeii	0.45	0.23	1.19	0.45	1.77	2.17	.	.	.	0.041	1.58	0.90	2.35
Vedde Ash	0.90	0.11	1.73	0.96	0.94	4.40	.	.	.	0.057	3.54	1.86	3.94
Reykjanes1226	0.68	0.05	2.15	1.62	1.65	1.03	.	.	.	0.038	1.19	2.30	3.84
Saksunarvatn	2.15	0.21	2.31	3.42	1.89	3.55	.	.	.	0.057	3.71	5.57	3.31
Cav-A	0.58	0.05	8.00	1.02	1.05	0.46	.	.	.	0.017	2.13	1.60	2.97
Tuhua	8.01	0.14	26.26	2.52	0.74	22.40	.	.	.	0.201	8.71	10.53	7.21
Armor1000	2.89	0.19	26.83	0.61	1.12	0.37	.	.	.	0.079	4.31	3.51	3.58
Katla1500	2.01	0.16	13.42	2.88	0.46	0.91	.	.	.	0.038	2.36	4.89	3.57
Reclus R ₁	10.31	0.19	9.03	13.12	0.18	18.05	0.04	0.31	0.60	0.000	0.01	23.47	N/A

*Electron Microprobe Analysis data is based on available data (overview Table 1; Fig. 1).

Table 4 Modeled dissolution parameters after alkaline (NaOH) extraction of heavy liquid separated a) volcanic glass shards and b) biogenic silica fractions. For each fraction ($Si_{Alk,x}$; wt% SiO_2) the Si/ Al_x ratios, rate of non-linear dissolution/release k_x (min^{-1}) for fraction x and b (wt% SiO_2 min^{-1}) the slope of the mineral dissolution with a Si/ Al_{min} ratio are given for all samples.

Sample	Volcanic glass shards						Biogenic Si							
	Fraction 1		Mineral		Total	$Si_{Alk,tot}$	Fraction 1		Fraction 2		Mineral		Total	
	$Si_{Alk,1}$	k_1	Si: Al_1	b	Si: Al_{min}		$Si_{Alk,1}$	k_1	Si: Al_1	$Si_{Alk,2}$	k_2	Si: Al_2	b	Si: Al_{min}
Hekla1991	3.45	0.58	20.08	0.049	1.92	3.45
EFJ2010_SJV	2.31	0.68	98.43	0.042	4.22	2.31
EFJ2010_1504	15.70	0.96	80.60	0.215	3.65	15.70
Vertical bFogo A	2.51	0.39	70.76	0.263	3.02	2.51
PAS 2T39	2.24	0.28	15.92	0.339	4.15	2.24
TC09_48a	1.25	0.65	42.51	0.294	3.81	1.25
Pompeii	22.59	0.90	110.64	0.027	1.45	22.59
Vedde Ash	0.54	1.27	657.58	0.031	3.78	0.54
Reykjanes1226	3.39	0.94	38.61	0.066	4.08	3.39
Saksunarvatn Cav-A	4.95	1.15	59.77	0.023	2.33	4.95	79.25	0.28	20504	79.25
Tuhua	3.80	0.71	142.89	0.023	2.59	3.80
Armor1000	3.84	0.19	17.00	0.206	6.59	3.84	23.50	0.47	390	30.38	0.05	7.50	.	53.88
Katla1500	1.82	0.43	371.55	0.097	2.53	1.82	79.78	0.37	361	79.78
Reclus R ₁	4.60	0.97	37.72	0.095	3.33	4.60	66.66	0.90	155	.	.	0.063	4.37	66.66
	77.33	0.23	111	77.33

Figures:

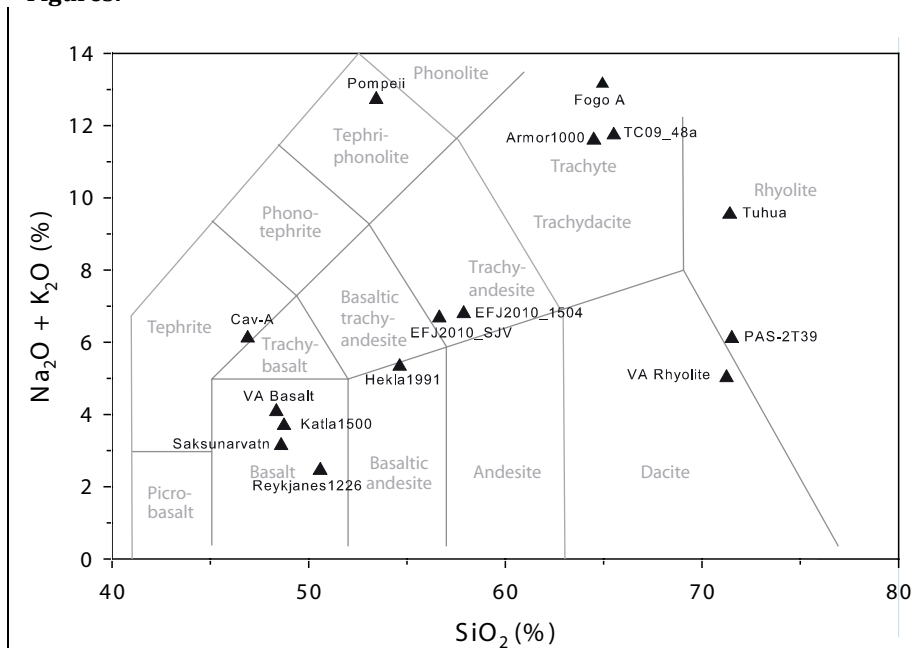


Figure 1 Composition of glass shards in our tephra samples presented on a total alkali silica diagram (SiO_2 vs. $\text{Na}_2\text{O} + \text{K}_2\text{O}$), [a standard classification used for pyroclastic volcanic rocks based on non-genetic features](#). Geochemical boundaries are according to Le Bas et al. (1986). Data are normalized averages of EMPA analysis. No data are available for Reclus R₁ Sample

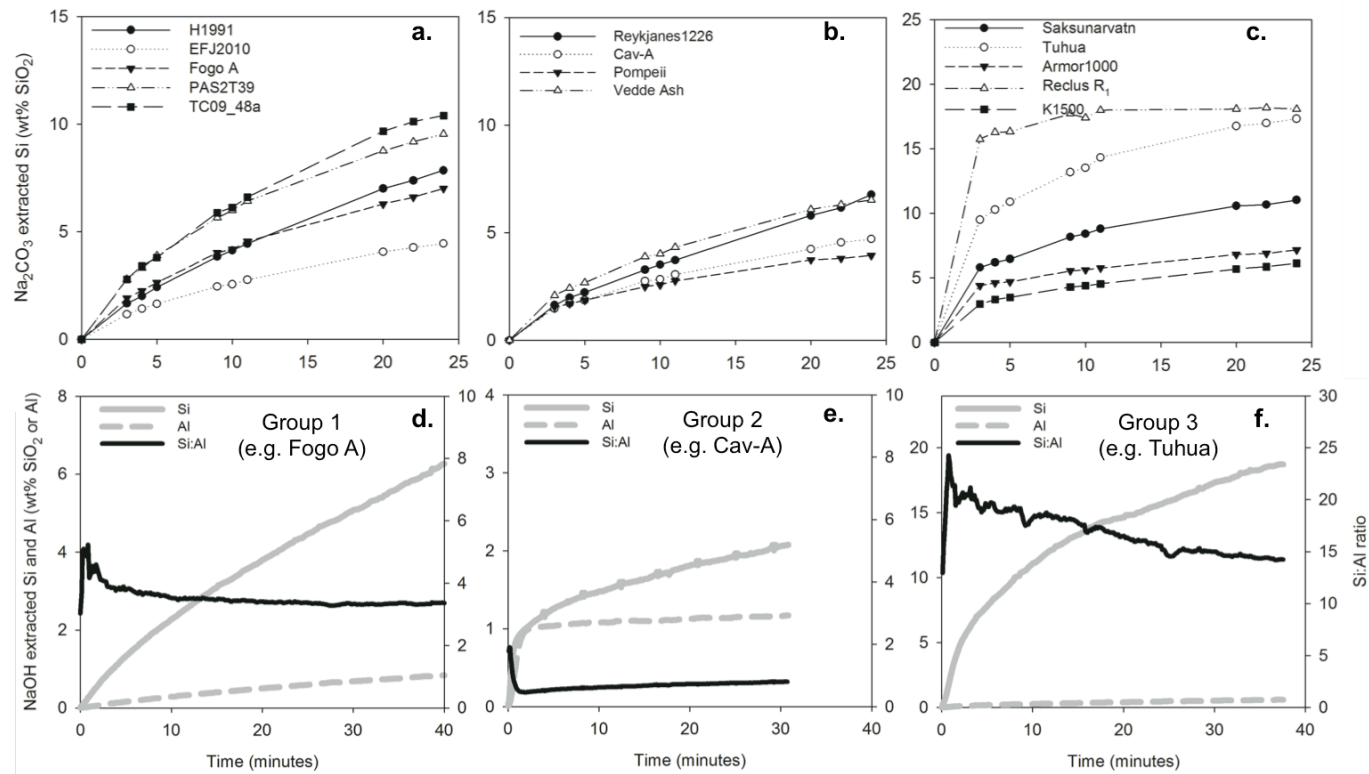


Figure 2 Dissolution curves of untreated tephra deposits grouped by characteristic features during the semi continuous extraction with Na₂CO₃(a-c) for Si and continuous extraction NaOH (d-f) for Si, Al and Si:Al ratio. Note: Groups are the same between methods but time unit x-axis differs between a-c and d-f. For NaOH only 1 representative curve per group is presented Group 1 contains Hekla1991, both EFJ2010, Fogo A, PAS-2T39 and TC09_48a; Group 2 contains Reykjanes1226, Cav-A, Pompeii and Vedde Ash; Group 3 contains Saksunarvatn, Tuhua, Armor1000, Katla1500 and Reclus R₁.

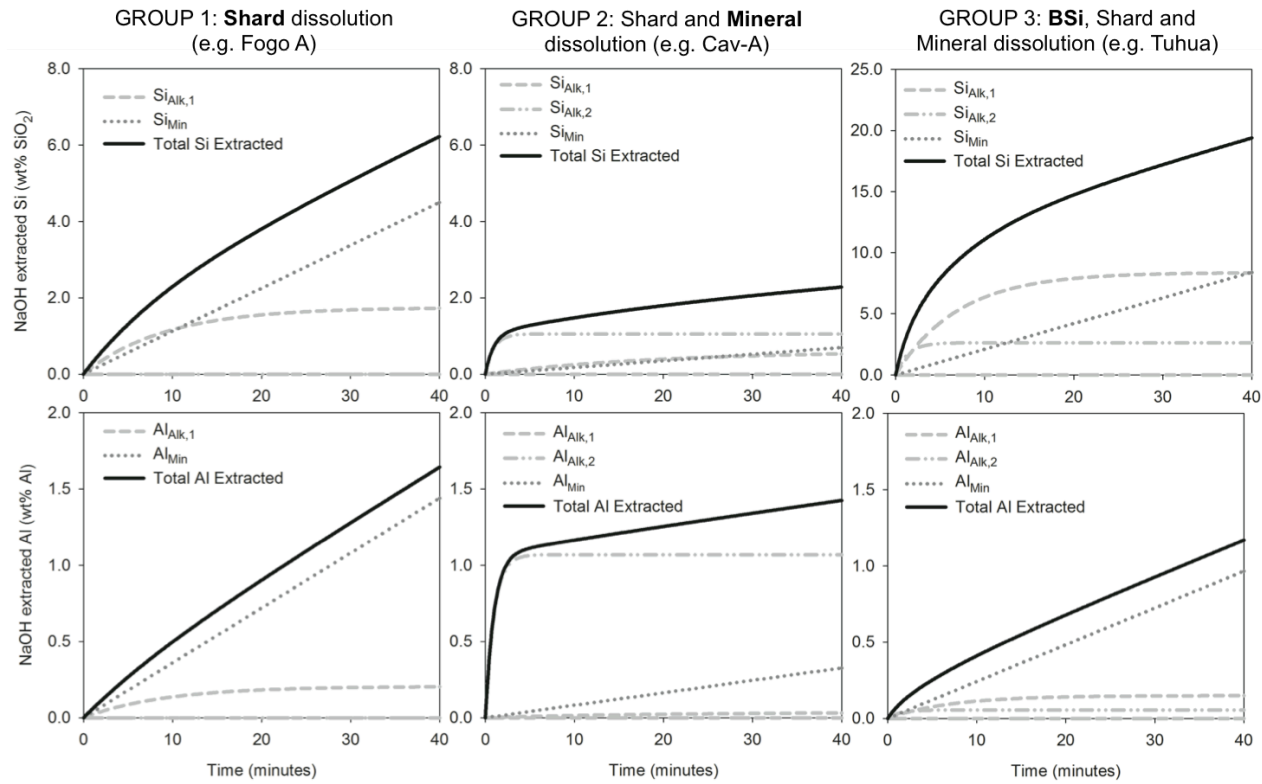


Figure 3 Separation in non-linear (Si_{Aik} & Al_{Aik}) and linear (Si_{Min} & Al_{Min}) fractions based modeling the continuous dissolution curves of Si and Al using Equation 1, grouped by their specific characteristics. Grouped by dominant fraction (in **bold**): Shards (solid circles), Minerals (open circles, i.e. nanocrystalline and clay minerals) or Biogenic Si (triangles). Group 1 contains Hekla1991, both EFJ2010, Fogo A PAS-2T39 and TC09_48a; Group 2 contains Reykjanes1226, Cav-A, Pompeii and Vedde Ash; Group 3 contains Saksunarvatn, Tuhua, Amor1000, Katla1500 and Reclus R₁.

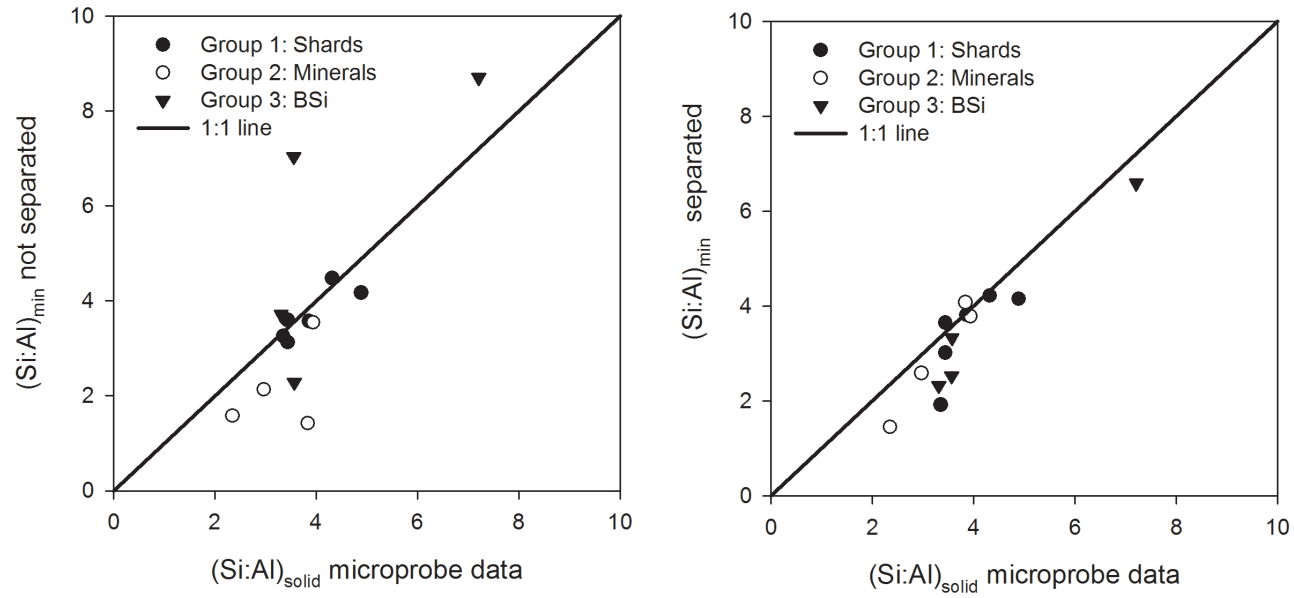


Figure 4 Comparison of $Si:Al_{solid}$ (from EMPA) and $Si:Al_{min}$ during alkaline dissolution (Table 3). Grouped by dominant fraction: Shards (solid circles), Minerals (open circles, i.e. nanocrystalline and clay minerals) or Biogenic Si (triangles). No data are available for Reclus R₁ Sample

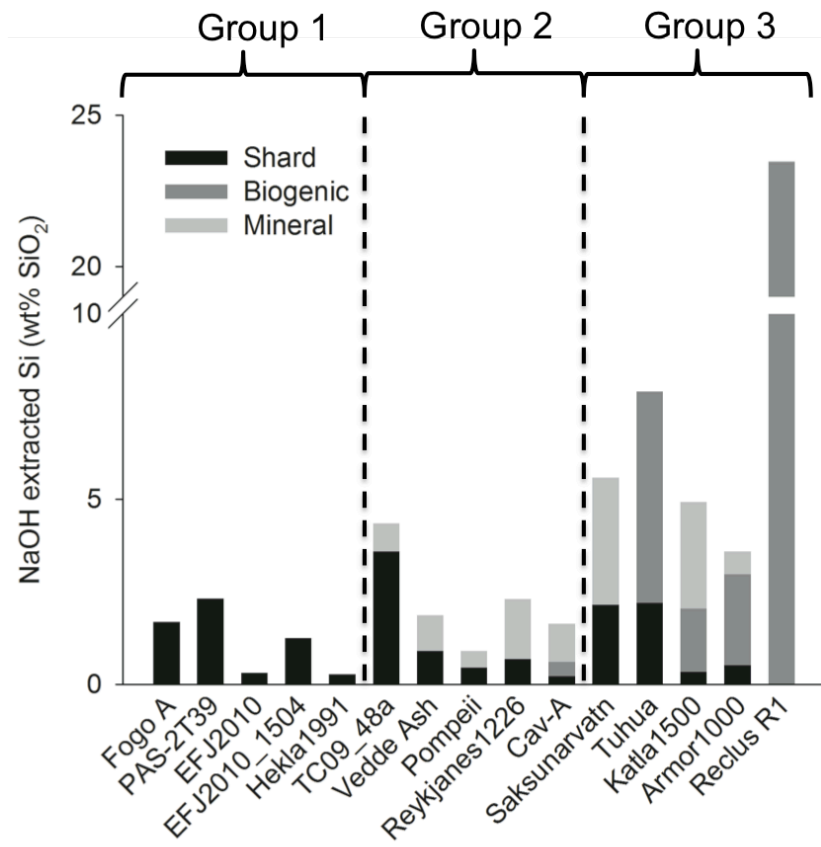


Figure 5 Separation of biogenic vs. non-biogenic (i.e. mineral or shard) fractions during alkaline extractions for all selected tephra deposits. Note: TC09_48a was reclassified to group 2 as it has a non-biogenic Si_{Aik} source.